Table 1. Patient Characteristics of Neuroblastoma Tissues with *ALK* Gene Gain or Amplification

Case	Age*	Primary tumor		Copy nos. of *ALK*‡	Amplification of N-*myc* (*n*)
		Location	Clinical stage†		
1	3y5m	Adrenal gland	IV	2.0 ± 0.2	+ (35)
2	5y0m	Peritoneum	IV	1.8 ± 0.1	+ (>150)
3	2y7m	Abdomen	IV	2.1 ± 0.8	+ (150)
4	8m	Adrenal gland	I	3.0 ± 1.0	–
5	4y9m	Abdomen	IV	2.0 ± 0.2	–
6	3y9m	Adrenal gland	III	2.7 ± 0.2	+ (>150)
7	1y4m	Adrenal gland	IV	2.8 ± 1.0	+ (150)
8	1y7m	Adrenal gland	IV	9.5 ± 2.2	+ (>100)

*Age of onset: year (y), month (m).
†The staging criterion was based on the International Neuroblastoma Staging System.
‡The averages of the calculated copy numbers from three independent blottings are shown.

30 minutes at room temperature. The cells were washed three times with PBS and mounted in glycerol-based 2.5% 1,4-diazabicyclo[2,2,2] octan. Confocal laser scanning analysis was carried out. For ALK/TUNEL, we first carried out TUNEL and then proceeded to standard immunocytochemistry using anti-ALK antibody. TUNEL was performed using the DeadEnd Fluorometric TUNEL System (Promega, Madison, WI) with the following modifications. The NB-39-nu cells seeded on the 24-well plates that were treated with siRNAs were washed with PBS twice and fixed with 4% paraformaldehyde (methanol free) for 25 minutes at 4°C. The cells were rinsed with PBS twice and then permeabilized with 0.2% Triton X-100 solution in PBS for 5 minutes at room temperature. The cells were washed with PBS twice and covered with an equilibration buffer (from the kit) for 10 minutes at room temperature. The equilibration buffer was drained off, and a reaction buffer containing the equilibration buffer, nucleotide mix, and terminal deoxynucleotidyl transferase enzyme was added to the cells and incubated at 37°C for 1 hour, avoiding exposure to light. The cells were incubated for 15 minutes at room temperature with 2× standard saline citrate to stop the reaction. The cells were washed with PBS three times and then stained for ALK using immunofluorescence as follows. The cells were blocked with 2% bovine serum albumin (Boehringer Mannheim, Germany) for 30 minutes at room temperature. The blocking solution was drained off, and the cells were incubated with a 1:1000 dilution of αALK for 1 hour at room temperature. The cells were rinsed with PBS three times and incubated with a 1:40 dilution of rhodamine-conjugated goat anti-rabbit secondary antibody (Santa Cruz Biotechnology) for 30 minutes at room temperature. The cells were washed three times with PBS and then mounted and observed in the same manner as that for ALK/TOTO-3.

DNA Extraction and Southern Blotting

Genomic DNAs derived from neuroblastoma cell lines were obtained from cultured cells as described using the procedure of Perucho et al.[29] Samples of 85 neuroblastoma tissues were collected at the Chiba Cancer Center and stored as forms of genomic DNA. The characteristics of some of these patients are shown in Table 1. The stage criterion was based on the International Neuroblastoma Staging System.[30] Samples of 5 μg of DNA digested by *Eco*RI were electrophoresed in 0.8% agarose gel and blotted onto nitrocellulose filters (Hybond-N+; Amersham, Piscataway, NJ). The probes for detecting the *ALK* gene, N-*myc* gene, and *ShcC* gene were used in our previous study.[27] The intensities of these signals were measured using a Molecular Imager FxPro (Bio-Rad). This study was approved by the ethical judging committee of the National Cancer Center and the Chiba Cancer Center of Japan.

RNA Interference Technique

Twenty-one-nucleotide double-stranded RNAs were synthesized and purified using Dharmacon Research (Lafayette, CO). To suppress the expression of ALK protein, two different pairs of ALK siRNAs, ALK-siRNA1 and ALK-siRNA2, were obtained. The sequences were 5′-GAGUCUGGCAGUUGACUUCdTdT-3′ for ALK-siRNA1 and 5′-GCUCCGGCGUGCCAAGCAGdTdT-3′ for ALK-siRNA2, corresponding to coding region 153 to 171 and 399 to 417 relative to the first nucleotide of the start codon, respectively. Entire sequences were derived from the sequence of human *ALK* mRNA (accession no. HSU62540). An siRNA, targeting a sequence in the firefly (*Photinus pyralis*) luciferase mRNA, was used as a negative control (Dharmacon) (luc-siRNA). We also used a scramble siRNA, Scramble Duplex II (Dharmacon) (s-siRNA) as a mismatch siRNA control in addition to luc-siRNA.

NB-39-nu cells were trypsinized, diluted with growth medium containing 10% fetal calf serum, and transferred to 12-well plates at 6×10^4 cells per well for 24 hours before transfection. The transfection of siRNA was carried out using jetSI (Poly plus transfection). A total of 100 μl of serum-free growth medium and 4 μl of jetSI per well were preincubated for 5 to 10 minutes at room temperature. While the incubation was being performed, 100 μl of serum-free growth medium was mixed with 5 μl of 20 μmol/L siRNA duplex (100 pmol). Total siRNA amounts of 50, 100, and 200 pmol were checked in preliminary experiments to find out 100 pmol is the minimal and optimal amount in this scale of RNAi. The 100 μl of jetSI serum-free medium solution was added to the 100 μl of siRNA

duplex solution, gently mixed, and incubated for 30 minutes at room temperature. The growth medium on the cells was removed, and 800 μl of serum-free medium was added to each well. A total of 200 μl of the entire mixture was overlaid onto the cells, and cells were incubated for 4 hours at 37°C in a 5% CO_2 incubator. After incubation, 1 ml of medium containing 4% fetal calf serum was added without removing the transfection mixture (final concentration 2%). The cells were assayed 84 hours after transfection. SK-N-MC cells were seeded in 12-well plates at a concentration of 1.3×10^5 cells per well. These were treated with siRNAs in the same way as NB-39-nu and assayed 48 hours after transfection. In the 24-well plate, the cells were seeded at the same concentration as the 12-well plate, and siRNAs and all other reagents were used at half volume. After transfection, the cells were examined under a light microscope every day.

Double Staining for ALK and TUNEL

For double staining, we first carried out TUNEL and then proceeded to standard immunocytochemistry using anti-ALK antibody. TUNEL was performed using the DeadEnd Fluorometric TUNEL System (Promega) with the following modifications. The NB-39-nu cells seeded on the 24-well plates that were treated with siRNAs were washed with PBS twice and fixed with 4% paraformaldehyde (methanol free) for 25 minutes at 4°C. The cells were rinsed with PBS twice and then permeabilized with 0.2% Triton X-100 solution in PBS for 5 minutes at room temperature. The cells were washed with PBS twice and covered with an equilibration buffer (from the kit) for 10 minutes at room temperature. The equilibration buffer was drained off, and a reaction buffer containing the equilibration buffer, nucleotide mix, and terminal deoxynucleotidyl transferase enzyme was added to the cells and incubated at 37°C for 1 hour, avoiding exposure to light. The cells were incubated for 15 minutes at room temperature with 2× standard saline citrate to stop the reaction. The cells were washed with PBS three times and then stained for ALK using immunofluorescence as follows. The cells were blocked with 2% bovine serum albumin (Boehringer Mannheim) for 30 minutes at room temperature. The blocking solution was drained off, and the cells were incubated with a 1:1000 dilution of αALK for 1 hour at room temperature. The cells were rinsed with PBS three times and incubated with a 1:40 dilution of rhodamine-conjugated goat anti-rabbit secondary antibody (Santa Cruz Biotechnology) for 30 minutes at room temperature. The cells were washed three times with PBS and mounted in glycerol-based 2.5% 1,4-diazabicyclo[2,2,2] octan. Confocal laser scanning analysis was carried out.

DNA Fragmentation Assay

To detect apoptotic DNA cleavage, DNA fragmentation assay was performed using an Apoptotic DNA Ladder kit (Chemicon International, Inc., Temecula, CA). The cells seeded on the 12-well plates that were treated with siRNAs as previously mentioned were collected in 1.5-ml microcentrifuge tubes. The cells were washed with PBS, centrifuged, and lysed with 20 μl of TE lysis buffer. The lysates were incubated with 5 μl of enzyme A (RNase A) at 37°C for 10 minutes and then at 55°C for 30 minutes after the addition of 5 μl of Enzyme B (Proteinase K). Afterward, 5 μl of ammonium acetate solution and 100 μl of absolute ethanol were added, and the samples were kept at −20°C for 10 minutes. The samples were centrifuged, and the pellets were washed with 70% ethanol. Then the DNA pellets were dissolved in 30 μl of DNA suspension buffer. DNA fragmentations were visualized by electrophoresis on 2% agarose gel containing ethidium bromide.

Immunohistochemistry

As for positive control, tumor xenograft was made by injection of NB-39-nu cells subcutaneously in 5-week-old SCID mice. Immunohistochemical staining with ALK antibody (αALK) (1:1000), was performed on 16 human neuroblastoma tumors selected from the surgical pathology file at the Department of Pathology, Aichi Medical University based on the results of histopathology evaluation[31] and N-*myc* status. All of those tumor samples were obtained before chemotherapy and irradiation therapy and included nine favorable histology cases with nonamplified N-*myc* (FH&NA), two unfavorable histology cases with amplified N-*myc* (UH&A), and five unfavorable histology cases with nonamplified N-*myc* (UH&NA).

Four-micrometer-thick sections from the formalin-fixed and paraffin-embedded tissue samples were deparaffinized and microwaved for three times for 5 minutes in Na-citrate buffer (pH 6.0) for antigen retrieval. The slides were first immersed in 0.3% hydrogen peroxide in methanol for 20 minutes and then in 10% normal goat serum for 30 minutes. The primary antibody (αALK) was then applied at 4°C overnight, followed by a standard staining procedure using the Vectastain ABC kit (Vector Laboratories, Burlingame, CA). Sections were counterstained with hematoxylin for light microscopic review and evaluation. ALK was always positively detected in the cytoplasm of NB-39-nu tumor xenograft and in the cytoplasm and neuritic processes of normal ganglion cells in the separate positive control sections as well as in the test sections as built-in control, whenever available. As for the negative controls, normal rabbit immunoglobulins (1:500 dilution; Vector Laboratories) or preimmune serum for α ALK (1:1000 dilution) was applied as the primary antibody.

Results

Significant Amplification of the ALK Gene and Constitutive Activation of ALK Kinase in Three Neuroblastoma Cell Lines

As shown in Figure 1A, NB-39-nu, Nagai, and NB-1 cells have significant levels of amplification of the *ALK* gene (30–40 copies per cell) among 25 neuroblastoma and neuroepithelioma cell lines examined. Other cell lines such as SK-N-MC have only one copy of the *ALK* gene just like the

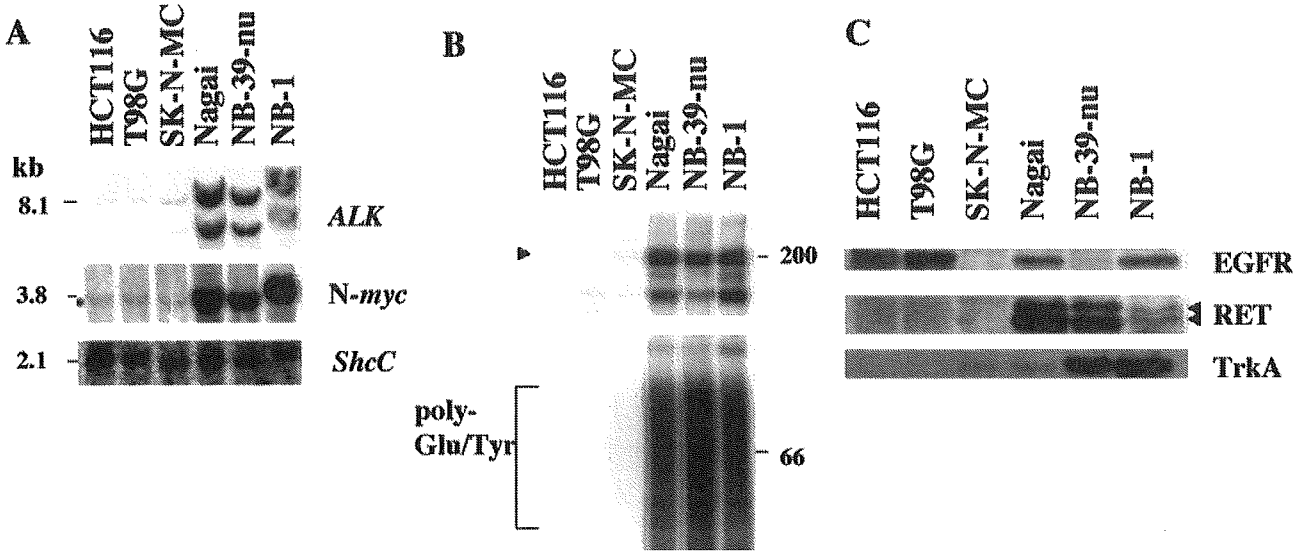

Figure 1. Marked gene amplification of the *ALK* locus and significant elevation of kinase activity of ALK in NB-39-nu, Nagai, and NB-1 cells. **A:** To detect ALK gene amplification, samples of 10 μg of DNA were digested with *Eco*RI. Fragments of about 2.5, 3.1, 6.1, and 8.1 kb were detected using the ^{32}P-labeled probe prepared as previously described.[27] Amplification of the N-*myc* gene was detected using the same filter re-hybridized with the probe for N-*myc*. As a control for the amounts of DNA, the same filter was re-hybridized with the probe for *ShcC*. **B:** *In vitro* kinase assay of ALK in neuroblastoma cells immunoprecipitated with αALK was performed as previously described.[27] Kinase reaction was performed without (**top panel**) or with (**bottom panel**) poly-Glu/Tyr (4:1) as exogenous substrates. Autophosphorylated ALK protein is marked by an **arrow**. Phosphorylated poly-Glu/Tyr is detected as smear indicated by the bracket. **C:** The expression patterns of other receptor tyrosine kinases in neuroblastoma cell lines. Each cell line was harvested, and about 30 μg of whole-cell lysates was subjected to Western blot analysis using the antibodies as indicated on the right. RET proteins are marked by **arrows**.

other types of solid tumor cell lines used as controls. *In vitro* kinase assay revealed outstanding ALK kinase activity in these three cell lines compared with other cells (Figure 1B), which is consistent with our previous study.[27] To examine whether overexpressed and activated ALK affects the expression of other RTKs in these cells, protein expression levels of RTKs, including EGFR, Ret, and TrkA, are compared with other cell lines. Significantly high levels of expression of EGFR and TrkA were observed in two of three cell lines overexpressing ALK (Figure 1C, top and bottom). Ret expression was commonly elevated in all three cell lines with activated ALK, especially in Nagai and NB-39-nu (Figure 1C, middle), consistent with previous study by Northern blotting.[32] Although it is unknown whether overexpression of these RTKs is related to overexpression of ALK, no obvious down-regulation of other RTKs was found in these *ALK*-amplified cell lines.

Inhibition of Activated ShcC, MAPKs, and Akt by Suppressing Activated ALK

To investigate the effect of suppressing the ALK expression level in *ALK*-amplified neuroblastoma cells using the RNAi technique, we synthesized two different RNA duplexes directed against nucleotide positions 153 to 171 and 399 to 417 within coding region *ALK* cDNA (ALK-siRNA1 and ALK-siRNA2, respectively). Because co-transfection of ALK-siRNA1 and ALK-siRNA2 was very effective in suppressing ALK expression, we performed all experiments presented here using a combination of two siRNAs, although similar results were obtained using only ALK-siRNA2. A sequence against the firefly luciferase gene (luc-siRNA) was used as a negative control. The expression of ALK protein is remarkably elevated in NB-39-nu and Nagai compared with other neuroblastoma cell lines, such as SK-M-MC (Figure 2A), caused by gene amplification.[27] The RNA duplexes were transfected into NB-39-nu cells with *ALK* gene amplification and SK-N-MC cells containing only a single copy of the *ALK* gene. We also tried to introduce ALK-siRNAs in several different neuroblastoma cell lines with or without *ALK* amplification in addition to NB-39-nu and SK-N-MC cells, resulting in partial or no reduction of ALK expression presumably due to the unsuccessful introduction in those cells. Therefore, we decided to use these two cell lines to perform further analysis of the effect of ALK knockdown by RNAi technique. RT-PCR analysis revealed that ALK mRNA level was reduced in both NB-39-nu cells and SK-N-MC cells treated with ALK-siRNAs, not in the cells treated with luc-siRNA and s-siRNA (Figure 2B). Both expression and phosphorylation of ALK kinase were significantly suppressed in the NB-39-nu cells treated with ALK-siRNAs compared with a mock-transfection control or cells treated with luc-siRNA (Figure 2C). In these cells, phosphorylation of ShcC was also suppressed despite the unchanged total amount of ShcC (Figure 2C), demonstrating that ShcC is a potent substrate of activated ALK kinase and that activation of ALK is actually responsible for the hyperphosphorylation of ShcC in these cancer cells. While the expression of downstream molecules, such as p44/42 MAPKs and Akt, was not affected by ALK-siRNAs, phosphorylation of these molecules was markedly reduced (Figure 2C). These results suggest that the Ras-MAPK pathway and the phosphatidylinositol 3-kinase/Akt pathway are dominantly regulated by activated ALK kinase in these cells. Interestingly, in SK-N-MC cells treated with ALK-siRNAs, phosphorylation levels of ShcC, p44/42 MAPKs, and Akt were not affected by

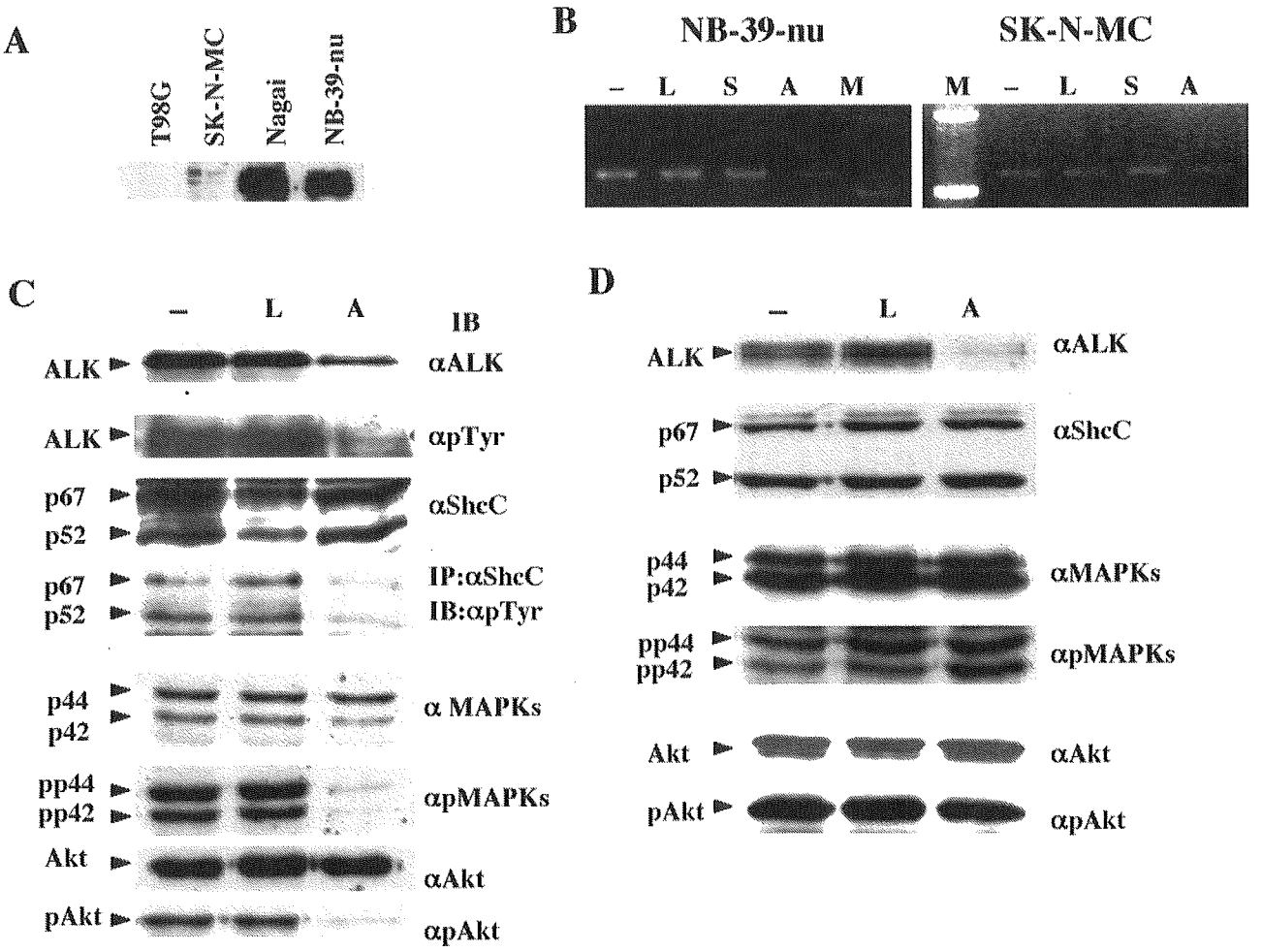

Figure 2. Suppression of ALK expression by siRNAs and changes in downstream molecules NB-39-nu cells and SK-N-MC cells. **A:** Expression levels of ALK protein in neuroblastoma cell lines including NB-39-nu and SK-N-MC. Each cell line was harvested, and about 30 μg of whole-cell lysates was subjected to Western blot analysis using αALK. **B:** mRNA levels of *Alk* in NB-39-nu cells. The cells were lysed at 84 hours after transfection and analyzed by RT-PCR. –, mock transfection; L, cells treated with luc-siRNA; S, cells treated with s-siRNA; A, cells treated with ALK-siRNAs; M, marker. **C:** NB-39-nu cells were harvested 84 hours after transfection. About 10 μg of whole-cell lysates or 250 μg of lysates immunoprecipitated with αShcC was subjected to Western blot analysis using the antibodies as indicated on the right. –, mock transfection; L, cells treated with luc-siRNA; A, cells treated with ALK-siRNAs. **D:** SK-N-MC cells were harvested 48 hours after transfection. About 10 μg of whole-cell lysates was subjected to Western blot analysis using the antibodies as indicated on the right. Bands of ShcC are marked by **arrows**. –, mock transfection; L, cells treated with luc-siRNA; A, cells treated with ALK-siRNAs.

ALK-siRNAs despite further suppression of the basal ALK expression level (Figure 2D), indicating that these pathways are not under the control of ALK in SK-N-MC cells.

Induction of Apoptosis by Suppression of Activated ALK

At 84 hours after transfection, apoptotic morphological changes, such as cell rounding, cytoplasmic blebbing, and irregularities of shape, were observed in NB-39-nu cells treated with ALK-siRNAs, whereas no significant changes were seen in the mock-transfected cells or in the luc-siRNA and the s-siRNA treated cells (Figure 3A). These morphological changes were not observed in SK-N-MC cells treated with ALK-siRNAs (data not shown). At 90 hours after transfection, NB-39-nu cells treated with ALK-siRNAs started to detach from the dish due to cell death.

To examine the localization of expression of ALK kinase, we performed double staining by anti-ALK antibody and TOTO-3, which stains the nucleus, in several neuroblastic cell lines. As shown in Figure 1D, unexpectedly, ALK protein overexpressed in NB-39-nu cells is localized in both membrane and cytoplasm. ALK staining was very weak in cell lines such as YT-nu and SK-N-MC with one copy of the *ALK* gene, however, its localization appeared to be the same as in NB-39-nu (data not shown). It was observed that the expression of ALK was completely lost after the RNAi-induced suppression of ALK (Figure 3C, top). To confirm whether the cell death resulted from apoptosis, cells were also analyzed by immunofluorescent TUNEL staining in NB-39-nu cells. TUNEL staining was clearly positive in these cells at 84 hours after transfection (Figure 3C, middle), indicating that apoptosis was induced in NB-39-nu cells treated with ALK-siRNAs. No significant TUNEL staining was observed in the mock-transfected cells or the luc-siRNA treated cells. Finally, DNA fragmentation assay was performed to measure the endonuclease activity accompa-

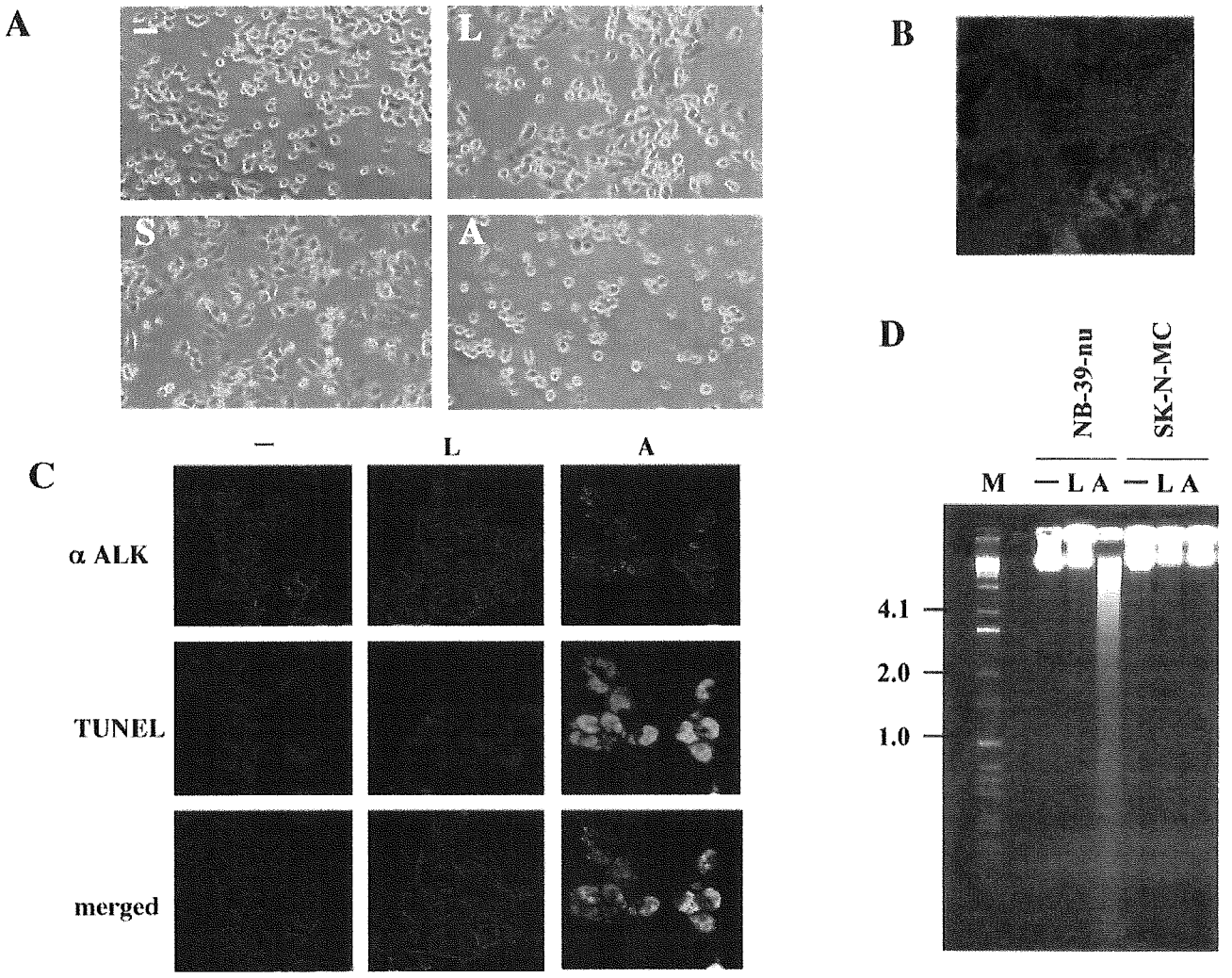

Figure 3. Induction of apoptosis in NB-39-nu cells treated with ALK-siRNAs. **A:** NB-39-nu cells on the dish were observed 84 hours after transfection under a light microscope. −, mock transfection; L, cells treated with luc-siRNA; S, cells treated with s-siRNA; A, cells treated with ALK-siRNAs. **B:** Cytoplasmic expression of ALK by immunocytostaining. The cells were stained for the expression of ALK (red) and apoptotic cells by TOTO-3 (blue). **C:** Cells on 24-well plates were fixed, and TUNEL assay was followed by staining with αALK (GST). The cells were stained for the expression of ALK (red) and apoptotic cells by TUNEL (green). −, mock transfection; L, cells treated with luc-siRNA; A, cells treated with ALK-siRNAs. **D:** DNA fragmentation assay in NB-39-nu cells and SK-N-MC cells treated with siRNAs. Genomic DNA was extracted 84 hours and 48 hours after transfection in NB-39-nu and in SK-N-MC, respectively. They were analyzed using electrophoresis. −, mock transfection; L, cells treated with luc-siRNA; A, cells treated with ALK-siRNAs; M, marker.

nied by apoptosis. The formation of significant DNA fragmentation was observed in the NB-39-nu cells but not in SK-N-MC cells treated with ALK-siRNAs (Figure 3D), indicating that cell apoptosis was induced through the suppression of ALK only in the NB-39-nu cells. This suggests that signaling pathways downstream of activated ALK dominantly regulate the survival of neuroblastoma cells with amplified ALK; therefore, the loss of ALK protein results in apoptotic changes to these cells.

Expression of ALK in Primary Neuroblastoma Tissues

Immunohistochemically, ALK was positively detected both in the cytoplasm of the neuroblastic cells and in the fine meshwork of neuropil of seven of nine tumors with favorable histology cases with nonamplified *N-myc* (FH&NA) (Figure 4, B and C). All seven unfavorable histology tumors (two UH&A tumors and five UH&NA tumors) were positive in the cytoplasm and/or in the fine meshwork of neuropil for ALK (Figure 4A). There was no correlation between the frequency or intensity of ALK-staining and histology of neuroblastoma tissues, showing majority of neuroblastoma samples showed a detectable amount of ALK. There was no significant staining using preimmune serum from the same rabbit as that for anti-ALK antibody (data not shown). Essentially the same results were obtained using a mouse monoclonal antibody against human ALK (ALK1: DAKO) (data not shown).

Amplification of the ALK Gene in Primary Neuroblastoma Tissues

It is essential to show whether ALK overexpression or gene amplification occurs in actual human neuroblastoma tissues in addition to neuroblastoma cell lines.

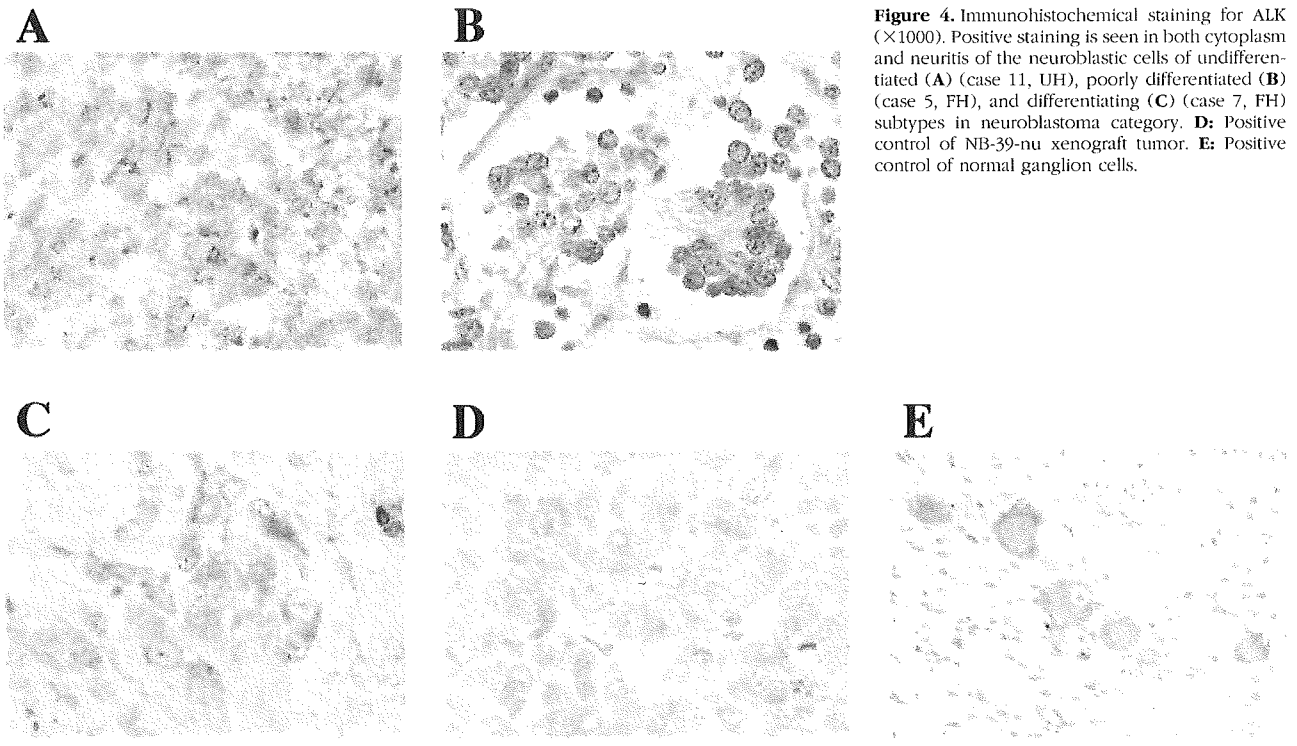

Figure 4. Immunohistochemical staining for ALK (×1000). Positive staining is seen in both cytoplasm and neuritis of the neuroblastic cells of undifferentiated (**A**) (case 11, UH), poorly differentiated (**B**) (case 5, FH), and differentiating (**C**) (case 7, FH) subtypes in neuroblastoma category. **D:** Positive control of NB-39-nu xenograft tumor. **E:** Positive control of normal ganglion cells.

Therefore, the mRNA amount of ALK kinase was first examined by RT-PCR on 32 primary neuroblastoma tissues (16 tissues with N-*myc* amplification and 16 tissues without N-*myc* amplification). Two of 32 cases showed slight elevation of *ALK* mRNA expression using several primer sets beyond the average expression level (data not shown).

To obtain more precise information about the copy numbers of *ALK*, we next analyzed the genomic DNAs of primary neuroblastoma tissues using Southern blot analysis. Whole purified DNA samples of tumors from 85 patients were examined. About the same number of N-*myc*-positive and N-*myc*-negative samples were collected to examine the relation between *Alk* and N-*myc* amplification. The intensities of signals on Southern blot membranes corresponding to the *ALK* gene and control *ShcC* gene, which is located on 9q22, were measured using a Molecular Imager FxPro (Bio-Rad), and the ratio of *ALK* signals to *ShcC* signals was calculated for each sample. Because more than 80% (70 samples) showed consistent ratios with each other in each experiment, these samples are treated as putative "single copy" controls. As several other samples showed apparently elevated intensity ratios, suggesting *ALK* amplification, relative copy numbers of *ALK* were calculated in comparison with average intensity ratios of putative single copy controls in each experiment. The results showed that there was significant *ALK* gene amplification in 8 of 85 patients (9.4%) (Figure 5). Seven of these eight cases, however, had only 1.8 to 3.0 copies of the *ALK* gene, suggesting a moderate gain of chromosomal focus rather than severe amplification. There was only one case that had outstanding amplification of ALK with approximately 10 copies. N-*myc* gene amplification was also detected in this case. The characteristics of the eight patients with *ALK* gain or amplification are shown in Table 1. Whereas seven of eight patients were classified as Stage III or IV (one as Stage III and six as Stage IV), the rest was classified as Stage I. The case with *ALK* amplification had N-*myc* amplification and was classified as Stage IV. Seven of eight patients were more than 1 year of age.

Discussion

Studies on ALK kinase demonstrate that activated ALK is involved in malignant tumor formation as forms of fusion proteins that force oligomerization of this kinase. We recently showed that the intact form of ALK protein is con-

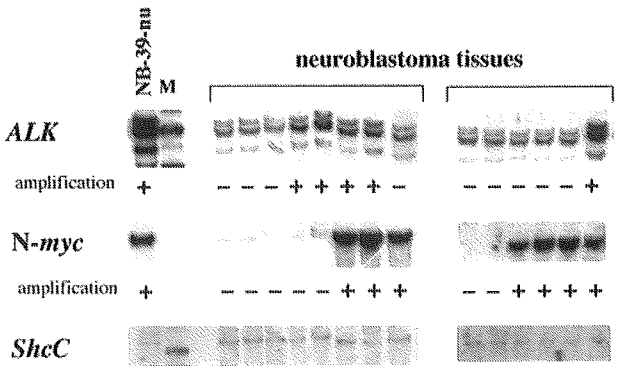

Figure 5. Detection of gene amplification of *ALK* and N-*myc* in primary neuroblastoma tissues. *ALK* was amplified in eight cases, and five of these eight cases are shown. The probe for *ALK* was removed from the filters, and the filters were re-hybridized in turn with other probes. Of eight cases with *ALK* amplification, N-*myc* amplification was detected in six cases and not detected in two cases. The probe for *ShcC* was used as a control for the amounts of DNA. M, marker.

stitutively activated by *ALK* gene amplification in three neuroblastoma cell lines, indicating a novel mechanism of activation of ALK kinase in malignancies.[27] In this study, amplification of the *ALK* gene was detected in primary neuroblastoma tissues for the first time. This suggests that activated ALK kinase plays a real role in the pathophysiology of neuroblastoma, such as giving a more malignant phenotype to the tumors by perturbing signal transduction. Recently, Motegi et al[33] showed that ALK transmits both mitogenic and differentiation signals, and that the MAPK pathway plays an important role in these effects in SK-N-SH cells without *ALK* gene amplification. Together with the fact that activated ALK surpasses regulation by other RTKs in cell lines with *ALK* gene amplification,[27] our new results showing apoptotic changes caused by the suppression of activated ALK protein clearly demonstrate the dominant role of ALK kinase in the survival of the *ALK*-amplified type of neuroblastoma.

The frequency and copy numbers of gene amplification of ALK were significantly lower in neuroblastic tumors compared with neuroblastic cell lines. Remarkable amplification of the *ALK* gene was detected in 1 tumor tissue of 85 tumor samples examined. Three neuroblastoma cell lines with *ALK* amplification had more than 30 copies of *ALK*, whereas primary neuroblastoma containing *ALK* gene amplification had within a range of 2 to 10 copies. This may be due to underestimation of the copy number in the tumor cells because of contamination of stromal cells and lymphocytes into the tumor tissues.[34,35] There may also be a mechanism in which cells with a higher copy number of *ALK* become the major population during the establishment of cell lines because of their growth advantage. Immunohistochemical analysis demonstrated, however, universal cytoplasmic expression of ALK in a wide range of neuroblastoma tumor samples, suggesting some transcriptional or posttranslational regulation of the ALK amount might exist in neuroblastoma cells. Although, due to the condition of the samples, we were unable to obtain information on the copy numbers of the *ALK* gene as for the samples used in the immunohistochemical analysis, further immunohistochemical screening may reveal neuroblastoma tissues with an outstanding amount of ALK protein because of gene amplification.

The N-*myc* gene was also amplified in this tumor and in all three cell lines with *ALK* amplification (NB-39-nu, Nagai, and NB-1). N-*myc* is located on 2p24.3 and *ALK* is on 2p23.2, suggesting that there is a tendency to synchronic amplification between N-*myc* and *ALK*. We were unable to conclude that there was an association between ALK amplification and prognosis mainly due to the limited number of positive samples and the short-term follow-up. Moreover, the *ALK* gene locus appears too far from the N-*myc* gene locus to be within a single amplicon. Further analysis in a greater number of samples with longer follow-up is necessary.

The activation of ALK results in hyperphosphorylation of ShcC in neuroblastoma cells, and NB-39-nu cells treated with ALK-siRNAs show suppressed tyrosine phosphorylation of ShcC, followed by apoptotic changes to these cells, suggesting that ShcC is a physiological substrate of the activated ALK kinase and that the ALK-ShcC pathway dominantly controls the survival of NB-39-nu cells even with the existence of other RTKs, such as EGFR, TrkA, and Ret. In neuronal cells, both ShcB (Sli/SCK) and ShcC (Rai/N-Shc) can bind activated RTKs, including the EGFR and Trk receptor.[36–39] Mice lacking both ShcB and ShcC exhibit a significant loss of sympathetic neurons, suggesting that ShcB and ShcC act in supporting sympathetic development and survival.[28] A recent study also showed that ShcC is a physiological substrate of Ret kinase and that it exerts a prosurvival function in neuronal cells.[40] Although high levels of TrkA expression correlate with a favorable outcome of neuroblastoma patients,[20] TrkA expression was significantly high in NB-39-nu and Nagai, which derive from tumors with a poor prognosis. This discrepancy may also be explained by the overwhelming control of cell survival by ALK kinase in these cell lines. Neuronal apoptosis is regulated through the action of critical protein kinase cascades, such as the phosphatidylinositol 3-kinase/Akt pathway and the Ras-MAPK pathway.[41,42] Apparently, neither pathway is properly controlled by EGF or nerve growth factor in NB-39-nu cells or Nagai cells.[27] Here, we also demonstrated that the suppression of activated ALK blocks MAPKs and Akt in these cells, resulting in apoptosis. On the other hand, the activity of MAPKs and Akt was not reduced by the suppression of a single copy of *ALK* in SK-N-MC cells. These results suggest that activation of ALK kinase completely remodeled the cellular signaling transduction pathways through ShcC so that cell survival entirely depended on signals originating from ALK kinase.

In conclusion, phosphorylation of several signaling molecules and cancer survival might be under the control of activated ALK kinase when gene amplification of ALK is as significant as in NB-39-nu cells, although the frequency of gene amplification in neuroblastoma tissues is not high. Cytoplasmic expression of ALK in neuroblastoma cells may suggest distinct function of this kinase in cell proliferation and survival. These findings further suggest that activated ALK kinase will be indispensable information for prognosis and treatment of neuroblastoma although the frequency is low.

References

1. Ullrich A, Schlessinger J: Signal transduction by receptors with tyrosine kinase activity. Cell 1990, 61:203–212
2. Heldin CH: Dimerization of cell surface receptors in signal transduction. Cell 1995, 80:213–223
3. Blume-Jensen P, Hunter T: Oncogenic kinase signalling. Nature 2001, 411:355–365
4. Pawson T: Protein modules and signalling networks. Nature 1995, 373:573–580
5. Kozlowski M, Larose L, Lee F, Le DM, Rottapel R, Siminovitch KA: SHP-1 binds and negatively modulates the c-Kit receptor by interaction with tyrosine 569 in the c-Kit juxtamembrane domain. Mol Cell Biol 1998, 18:2089–2099
6. Morris SW, Kirstein MN, Valentine MB, Dittmer KG, Shapiro DN, Saltman DL, Look AT: Fusion of a kinase gene ALK, to a nucleolar protein gene NPM, in non-Hodgkin's lymphoma. Science 1994, 263:1281–1284

7. Shiota M, Fujimoto J, Semba T, Satoh H, Yamamoto T, Mori S: Hyperphosphorylation of a novel 80 kDa protein-tyrosine kinase similar to Ltk in a human Ki-1 lymphoma cell line, AMS3. Oncogene 1994, 9:1567–1574
8. Bridge JA, Kanamori M, Ma Z, Pickering D, Hill DA, Lydiatt W, Lui MY, Colleoni GW, Antonescu CR, Ladanyi M, Morris SW: Fusion of the ALK gene to the clathrin heavy chain gene, CLTC, in inflammatory myofibroblastic tumor. Am J Pathol 2001, 159:411–415
9. Iwahara T, Fujimoto J, Wen D, Cupples R, Bucay N, Arakawa T, Mori S, Ratzkin B, Yamamoto T: Molecular characterization of ALK, a receptor tyrosine kinase expressed specifically in the nervous system. Oncogene 1997, 14:439–449
10. Morris SW, Naeve C, Mathew P, James PL, Kirstein MN, Cui X, Witte DP: ALK, the chromosome 2 gene locus altered by the t(2;5) in non-Hodgkin's lymphoma, encodes a novel neural receptor tyrosine kinase that is highly related to leukocyte tyrosine kinase (LTK). Oncogene 1997, 14:2175–2188
11. Ben-Neriah Y, Bauskin AR: Leukocytes express a novel gene encoding a putative transmembrane protein-kinase devoid of an extracellular domain. Nature 1988, 333:672–676
12. Maru Y, Hirai H, Takaku F: Human ltk: gene structure and preferential expression in human leukemic cells. Oncogene Res 1990, 5:199–204
13. Bernards A, de la Monte SM: The ltk receptor tyrosine kinase is expressed in pre-B lymphocytes and cerebral neurons and uses a non-AUG translational initiator. EMBO J 1990, 9:2279–2287
14. Pulford K, Lamant L, Morris SW, Butler LH, Wood KM, Stroud D, Delsol G, Mason DY: Detection of anaplastic lymphoma kinase (ALK) and nucleolar protein nucleophosmin (NPM)-ALK proteins in normal and neoplastic cells with the monoclonal antibody ALK1. Blood 1997, 89:1394–1404
15. Shiota M, Fujimoto J, Takenaga M, Satoh H, Ichinohasama R, Abe M, Nakano M, Yamamoto T, Mori S: Diagnosis of t(2;5)(p23;q35)-associated Ki-1 lymphoma with immunohistochemistry. Blood 1994, 84:3648–3652
16. Duyster J, Bai RY, Morris SW: Translocations involving anaplastic lymphoma kinase (ALK). Oncogene 2001, 20:5623–5637
17. Stoica GE, Kuo A, Aigner A, Sunitha I, Souttou B, Malerczyk C, Caughey DJ, Wen D, Karavanov A, Riegel AT, Wellstein A: Identification of anaplastic lymphoma kinase as a receptor for the growth factor pleiotrophin. J Biol Chem 2001, 276:16772–16779
18. Stoica GE, Kuo A, Powers C, Bowden ET, Sale EB, Riegel AT, Wellstein A: Midkine binds to anaplastic lymphoma kinase (ALK) and acts as a growth factor for different cell types. J Biol Chem 2002, 277:35990–35998
19. Evans AE, D'Angio GJ, Randolph J: A proposed staging for children with neuroblastoma: children's cancer study group A. Cancer 1971, 27:374–378
20. Nakagawara A, Arima-Nakagawara M, Scavarda NJ, Azar CG, Cantor AB, Brodeur GM: Association between high levels of expression of the TRK gene and favorable outcome in human neuroblastoma. N Engl J Med 1993, 328:847–854
21. Nakagawara A, Azar CG, Scavarda NJ, Brodeur GM: Expression and function of TRK-B and BDNF in human neuroblastomas. Mol Cell Biol 1994, 14:759–767
22. Nakagawara A, Nakamura Y, Ikeda H, Hiwasa T, Kuida K, Su MS, Zhao H, Cnaan A, Sakiyama S: High levels of expression and nuclear localization of interleukin-1 beta converting enzyme (ICE) and CPP32 in favorable human neuroblastomas. Cancer Res 1997, 57:4578–4584
23. Posmantur R, McGinnis K, Nadimpalli R, Gilbertsen RB, Wang K: Characterization of CPP32-like protease activity following apoptotic challenge in SH-SY5Y neuroblastoma cells. J Neurochem 1997, 68:2328–2337
24. Adida C, Berrebi D, Peuchmaur M, Reyes-Mugica M, Altieri DC: Anti-apoptosis gene, survivin, and prognosis of neuroblastoma. Lancet 1998, 351:882–883
25. Hiyama E, Hiyama K, Yokoyama T, Matsuura Y, Piatyszek MA, Shay JW: Correlating telomerase activity levels with human neuroblastoma outcomes. Nat Med 1995, 1:249–255
26. Lamant L, Pulford K, Bischof D, Morris SW, Mason DY, Delsol G, Mariame B: Expression of the ALK tyrosine kinase gene in neuroblastoma. Am J Pathol 2000, 156:1711–1721
27. Miyake I, Hakomori Y, Shinohara A, Gamou T, Saito M, Iwamatsu A, Sakai R: Activation of anaplastic lymphoma kinase is responsible for hyperphosphorylation of ShcC in neuroblastoma cell lines. Oncogene 2002, 21:5823–5834
28. Sakai R, Henderson JT, O'Bryan JP, Elia AJ, Saxton TM, Pawson T: The mammalian ShcB and ShcC phosphotyrosine docking proteins function in the maturation of sensory and sympathetic neurons. Neuron 2000, 28:819–833
29. Perucho M, Goldfarb M, Shimizu K, Lama C, Fogh J, Wigler M: Human-tumor-derived cell lines contain common and different transforming genes. Cell 1981, 27:467–476
30. Brodeur GM, Pritchard J, Berthold F, Carlsen NL, Castel V, Castelberry RP, De Bernardi B, Evans AE, Favrot M, Hedborg F, Kaneko M, Kemshead J, Lampert F, Lee RE, Look AT, Pearson AD, Philip T, Roald B, Sawada T, Seeger RC, Tsuchida Y, Voute PA: Revisions of the international criteria for neuroblastoma diagnosis, staging, and response to treatment. J Clin Oncol 1993, 11:1466–1477
31. Shimada H, Ambros IM, Dehner LP, Hata J, Joshi VV, Roald B, Stram DO, Gerbing RB, Lukens JN, Matthay KK, Castleberry RP: The International Neuroblastoma Pathology Classification (the Shimada system). Cancer 1999, 86:364–372
32. Ikeda I, Ishizaka Y, Tahira T, Suzuki T, Onda M, Sugimura T, Nagao M: Specific expression of the ret proto-oncogene in human neuroblastoma cell lines. Oncogene 1990, 5:1291–1296
33. Motegi A, Fujimoto J, Kotani M, Sakuraba H, Yamamoto T: ALK receptor tyrosine kinase promotes cell growth and neurite outgrowth. J Cell Sci 2004, 117:3319–3329
34. Slamon DJ, Clark GM, Wong SG, Levin WJ, Ullrich A, McGuire WL: Human breast cancer: correlation of relapse and survival with amplification of the HER-2/neu oncogene. Science 1987, 235:177–182
35. Tsuda H, Hirohashi S, Shimosato Y, Hirota T, Tsugane S, Yamamoto H, Miyajima N, Toyoshima K, Yamamoto T, Yokota J, Yoshida T, Sakamoto H, Terada M, Sugimura T: Correlation between long-term survival in breast cancer patients and amplification of two putative oncogene-coamplification units: hst-1/int-2 and c-erbB-2/ear-1. Cancer Res 1989, 49:3104–3108
36. Ganju P, O'Bryan JP, Der C, Winter J, James IF: Differential regulation of SHC proteins by nerve growth factor in sensory neurons and PC12 cells. Eur J Neurosci 1998, 10:1995–2008
37. Nakamura T, Komiya M, Gotoh N, Koizumi S, Shibuya M, Mori N: Discrimination between phosphotyrosine-mediated signaling properties of conventional and neuronal Shc adapter molecules. Oncogene 2002, 21:22–31
38. Nakamura T, Muraoka S, Sanokawa R, Mori N: N-Shc and Sck, two neuronally expressed Shc adapter homologs: their differential regional expression in the brain and roles in neurotrophin and Src signaling. J Biol Chem 1998, 273:6960–6967
39. O'Bryan JP, Songyang Z, Cantley L, Der CJ, Pawson T: A mammalian adaptor protein with conserved Src homology 2 and phosphotyrosine-binding domains is related to Shc and is specifically expressed in the brain. Proc Natl Acad Sci USA 1996, 93:2729–2734
40. Pelicci G, Troglio F, Bodini A, Melillo RM, Pettirossi V, Coda L, De Giuseppe A, Santoro M, Pelicci PG: The neuron-specific Rai (ShcC) adaptor protein inhibits apoptosis by coupling Ret to the phosphatidylinositol 3-kinase/Akt signaling pathway. Mol Cell Biol 2002, 22:7351–7363
41. Yuan J, Yankner BA: Apoptosis in the nervous system. Nature 2000, 407:802–809
42. De Vita G, Melillo RM, Carlomagno F, Visconti R, Castellone MD, Bellacosa A, Billaud M, Fusco A, Tsichlis PN, Santoro M: Tyrosine 1062 of RET-MEN2A mediates activation of Akt (protein kinase B) and mitogen-activated protein kinase pathways leading to PC12 cell survival. Cancer Res 2000, 60:3727–3731

Behavioral/Systems/Cognitive

Hippocampal Synaptic Modulation by the Phosphotyrosine Adapter Protein ShcC/N-Shc via Interaction with the NMDA Receptor

Yoshiaki Miyamoto,[1] Ling Chen,[2] Masahiro Sato,[1] Masahiro Sokabe,[2,3] Toshitaka Nabeshima,[4] Tony Pawson,[5] Ryuichi Sakai,[6] and Nozomu Mori[1,7]

[1]Department of Molecular Genetics, National Institute for Longevity Sciences, Oobu 474-8522, Japan, [2]Cell Mechanosensing Project, International Cooperative Research Project–Japan Science and Technology Agency, and Departments of [3]Physiology and [4]Neuropsychopharmacology and Hospital Pharmacy, Nagoya University Graduate School of Medicine, Nagoya 466-8560, Japan, [5]Department of Molecular and Medical Genetics, University of Toronto, Toronto, Ontario M5S 1A8, Canada, [6]Growth Factor Division, National Cancer Center Research Institute, Tokyo 104-0045, Japan, and [7]Department of Anatomy and Neurobiology, Nagasaki University School of Medicine, Nagasaki 852-8523, Japan

N-Shc (neural Shc) (also ShcC), an adapter protein possessing two phosphotyrosine binding motifs [PTB (phosphotyrosine binding) and SH2 (Src homology 2) domains], is predominantly expressed in mature neurons of the CNS and transmits neurotrophin signals from the TrkB receptor to the Ras/mitogen-activated protein kinase (MAPK) pathway, leading to cellular growth, differentiation, or survival. Here, we demonstrate a novel role of ShcC, the modulation of NMDA receptor function in the hippocampus, using *ShcC* gene-deficient mice. In behavioral analyses such as the Morris water maze, contextual fear conditioning, and novel object recognition tasks, ShcC mutant mice exhibited superior ability in hippocampus-dependent spatial and nonspatial learning and memory. Consistent with this finding, electrophysiological analyses revealed that hippocampal long-term potentiation in ShcC mutant mice was significantly enhanced, with no alteration of presynaptic function, and the effect of an NMDA receptor antagonist on its expression in the mutant mice was notably attenuated. The tyrosine phosphorylation of NMDA receptor subunits NR2A and NR2B was also increased, suggesting that ShcC mutant mice have enhanced NMDA receptor function in the hippocampus. These results indicate that ShcC not only mediates TrkB-Ras/MAPK signaling but also is involved in the regulation of NMDA receptor function in the hippocampus via interaction with phosphotyrosine residues on the receptor subunits and serves as a modulator of hippocampal synaptic plasticity underlying learning and memory.

Key words: ShcC/N-Shc; phosphotyrosine adapter protein; learning and memory; long-term potentiation; hippocampus; NMDA receptor

Introduction

Long-term potentiation (LTP) in the hippocampus, a well characterized form of activity-dependent synaptic plasticity, serves as a major cellular mechanism of learning and memory (Bliss and Collingridge, 1993; Malenka and Nicoll, 1999). The NMDA and AMPA types of glutamate receptors (GluRs) play critical roles in the induction of hippocampal LTP (Tsien et al., 1996; Zamanillo et al., 1999). In addition to the primary importance of the glutamate receptors, it has been reported that neurotrophins, particularly brain-derived neurotrophic factor (BDNF), modulate the maintenance of hippocampal LTP through the activation of TrkB receptor tyrosine kinases (Poo, 2001; Lu, 2003). Also, a variety of intracellular signaling cascades, including the Ras/mitogen-activated protein kinase (MAPK) pathway, are reported to influence LTP formation (Ohno et al., 2001; Silva, 2003).

The BDNF-activated TrkB receptors recruit various adapter proteins such as Shc, Frs-2, and phospholipase-Cγ (PLCγ). The adapter proteins are tyrosine phosphorylated by the activated TrkB receptors and determine the flow of downstream intracellular signaling cascades to cellular growth, differentiation, or survival. Binding of Shc or Frs-2 leads to the activation of Ras/MAPK and PI3K (phosphoinositide-3 kinase)/Akt pathways, whereas binding of PLCγ stimulates the release of intracellular Ca^{2+} via inositol 1,4,5-trisphosphate (IP3) and thereby activates the Ca^{2+}–calmodulin-dependent kinase IV (CaMKIV) pathway (Kaplan and Miller, 2000; Patapoutian and Reichardt, 2001). Therefore, it is hypothesized that TrkB-Ras/MAPK signaling plays a role in the hippocampal LTP underlying learning and memory (Adams and Sweatt, 2002; Ying et al., 2002).

The Shc family consists of ShcA/Shc (p66, p52, and p46 isoforms), ShcB/Sck (p68), and ShcC/neural Shc (N-Shc) (p69 and p55), and possesses two modular regions that bind to phosphorylated tyrosine-containing peptide motifs: a PTB (phosphoty-

Received March 3, 2004; revised Dec. 30, 2004; accepted Jan. 3, 2005.

The initial part of this work was supported by the program "Protecting the Brain" of the Core Research for Evolutional Science and Technology–Japan Science and Technology Agency, and later, in part, by a Virtual Research Institute of Aging fund of Nippon Boehringer Ingelheim, the Uehara Memorial Research Fund, Funds for Comprehensive Research on Aging and Health from Ministry of Health, Labor, and Welfare, and grants-in-aid from the Ministry of Education, Culture, Sports, Science, and Technology of Japan. We thank Dr. T. Nakamura for valuable advice and I. Nakano and Y. Kadokawa for technical assistance and laboratory maintenance.

Correspondence should be addressed to Dr. Nozomu Mori, Department of Anatomy and Neurobiology, Nagasaki University School of Medicine, 1-12-4 Sakamoto, Nagasaki 852-8523, Japan. E-mail: morinosm@net.nagasaki-u.ac.jp.

DOI:10.1523/JNEUROSCI.3030-04.2005

 0270-6474/05/251826-10$15.00/0

rosine binding) domain and an SH2 (Src homology 2) domain. All of the Shc family members serve to link a number of receptor tyrosine kinases with multiple intracellular signaling cascades. ShcA is widely expressed in most tissues, whereas both ShcB and ShcC are predominantly expressed in the nervous system (Cattaneo and Pelicci, 1998; Ravichandran, 2001). The brain-enriched ShcC would be in a good position to modulate the hippocampal LTP via regulation of TrkB-Ras/MAPK signaling, because it has been implicated in the BDNF-TrkB signaling toward the Ras/MAPK pathway in cultured cells (Nakamura et al., 1998; Liu and Meakin, 2002).

Recent studies revealed that the so-called "Shc site" of the TrkB receptor (Tyr^{515}) was not relevant to the hippocampal LTP, because mice with a targeted point mutation of the TrkB–Shc site showed apparently no significant change in LTP formation (Korte et al., 2000; Minichiello et al., 2002). These findings are in contrast to the aforementioned hypothesis pointing to a role for TrkB-Ras/MAPK signaling in the hippocampal LTP. Accordingly, in the present study, we attempted to clarify whether the phosphotyrosine adapter protein *ShcC*, which binds the TrkB–Shc site leading to the Ras/MAPK pathway, is involved in hippocampal functions, using *ShcC* gene-deficient mice. Based on the results presented herein, we propose a novel role for ShcC in hippocampal synaptic plasticity, as evidenced by the enhancement of hippocampal LTP and hippocampus-dependent learning and memory in ShcC mutant mice.

Materials and Methods

Animals. Mice lacking ShcC were generated by Sakai et al. (2000). The homozygous mutant mice (−/−; 3 months of age) and the littermate 2 wild-type mice (+/+; 3 months of age) were obtained by crossing F2 heterozygous mutant mice (+/−). The genotypes of mice were determined by Southern blot analyses of tail DNA. C57BL/6 mice (Nihon SLC, Hamamatsu, Japan) were used for biochemical analyses of the Shc family members. The mice were housed in plastic cages and were kept in a regulated environment (24 ± 1°C; 50 ± 5% humidity), with a 12 h light/dark cycle (lights on at 9:00 A.M.). Food and tap water were available *ad libitum*. All of the experiments were performed in accordance with the Guidelines for Animal Experiments of the Nagoya University School of Medicine. The procedures involving animals and their care were conducted in conformity with the international guidelines *Principles of Laboratory Animal Care* (National Institutes of Health publication 85-23, revised 1985).

Plasmids and antibodies. Plasmids encoding cDNAs of mouse p52-ShcA, p68-ShcB, and p55-ShcC were as described previously (Kojima et al., 2001) and were epitope-tagged with T7 at the N terminus. Antibodies against ShcA (catalog #S68020) and ShcC (S55720) were obtained from Transduction Laboratories (San Diego, CA). Antibody against ShcB was prepared as described previously (Sakai et al., 2000). Anti-phosphotyrosine antibody (catalog #05-321) was purchased from Upstate Biotechnology (Charlottesville, VA). Antibodies against NR1 (catalog #sc-9058), NR2A (catalog #sc-9056), NR2B (catalog #sc-9057), postsynaptic density 95 (PSD95) (catalog #sc-6926), Src (catalog #sc-5266), Fyn (catalog #sc-434), and the Src family (catalog #sc-18) were from Santa Cruz Biotechnology (Santa Cruz, CA). Anti-phospho-Src family (Tyr^{418}) antibody (catalog #44-660) was purchased from Biosource (Camarillo, CA).

Northern blot analysis. Total RNAs were isolated using TRIzol reagents (Invitrogen, Carlsbad, CA). Isolated total RNAs (20 μg) were electrophoresed on a formalin/agarose gel and blotted onto a positively charged nylon membrane. Specific cDNA probes for the Shc family members were made by Megaprime DNA labeling systems and [α-^{32}P]dCTP (Amersham Biosciences, Piscataway, NJ) and purified with NucTrap Probe Purification Columns (Stratagene, La Jolla, CA). Membranes were hybridized with the ^{32}P-labeled cDNA probes as described previously (Nakamura et al., 1998).

In situ *hybridization analysis.* Mouse brain sections (15 μm) were cut on a cryostat, thaw-mounted on poly-L-lysine-coated slides, and stored at −80°C until use. The frozen brain sections were brought to room temperature and air-dried. The sections were postfixed with 4% paraformaldehyde in 0.1 M phosphate buffer, acetylated with 0.25% acetic anhydride in 0.1 M triethanolamine, and dehydrated through an ascending series of ethanol concentrations. To prepare antisense and sense cRNA probes, the plasmids encoding cDNA of ShcA, ShcB, or ShcC were linearized by cutting at a single site (antisense, *Eco*RI; sense, *Hin*dIII). *In vitro* transcription was performed using RNA polymerase (antisense, T7 RNA polymerase; sense, SP6 RNA polymerase) and [α-^{35}S]UTP (ICN Biomedicals, Costa Mesa, CA). *In situ* hybridization with the ^{35}S-labeled cRNA probes was performed as described previously (Nakamura et al., 1998). The sections were counterstained with thionine and dehydrated. The images were captured by the HC-2000 video camera system (Fuji Photo Film, Tokyo, Japan) and reconstructed using computer software.

Western blot analysis and immunoprecipitation assay. Mouse brains were homogenized in a lysis buffer [50 mM Tris-HCl, pH 7.5, 150 mM NaCl, 5 mM EDTA, 10 mM NaF, 1 mM sodium orthovanadate, 1% Triton X-100, 0.5% sodium deoxycholate, 1 mM phenylmethylsulfonyl fluoride, and protease inhibitor mixture (Complete; Roche, Mannheim, Germany)] or a modified lysis buffer containing 0.1% SDS for immunoprecipitation assays. For Western blot analysis, total proteins (10 μg) were separated by SDS-PAGE and blotted onto a polyvinylidene difluoride (PVDF) membrane. For immunoprecipitation assays, total proteins (500 μg) were incubated with an appropriate antibody and then protein G-Sepharose was added and further incubated. The immunoprecipitates were recovered by centrifugation and resuspended in a sample buffer. The samples (10 μl) were separated by electrophoresis and blotted onto a PVDF membrane. The membranes were incubated with primary antibodies, and proteins were detected by HRP-conjugated secondary antibodies using the ECL detection kit (Amersham Biosciences).

Histological analysis. Mouse brains were perfused with 4% paraformaldehyde in PBS and removed. Sections (15 μm) were cut, mounted on slides, and stored at −80°C until use. Nissl staining was done according to standard procedures. The images were captured with an HC-2000 video camera system. For immunochemical staining, the sections were permeabilized with 0.2% Triton X-100, blocked with 3% BSA, and incubated with antibody against microtubule-associated protein 2 (MAP2) (catalog #M1406; Sigma, St. Louis, MO). To detect specific signals for MAP2, the sections were incubated with Alexa Fluor 488-conjugated secondary antibody (catalog #A-11029; Molecular Probes, Eugene, OR). Fluorescence images were obtained with the confocal imaging system Micro Radiance (Bio-Rad Laboratories, Hercules, CA).

Behavioral analysis. To measure locomotor activity, a mouse was placed in a transparent acrylic cage with a black Plexiglas floor (45 × 26 × 40 cm), and locomotion and rearing were measured for 60 min using infrared counters (Scanet SV-10; Toyo Sangyo, Toyama, Japan).

To measure nociceptive responses to electric footshock, a mouse was placed in a transparent Plexiglas cage with a grid floor for footshock (25 × 30 × 11 cm) and an ascending footshock series (0.01, 0.02, 0.03, 0.04, 0.05, 0.06, 0.08, 0.10, 0.13, 0.16, 0.20, 0.25, 0.30, 0.40, 0.50, and 0.60 mA for 0.5 s; 30 s interval) was delivered through an electric shock generator (NS-SG01; Neuroscience, Tokyo, Japan). The electric current needed to elicit first flinching, vocalizing, or jumping behavior was recorded as the footshock threshold.

For the Morris water maze task, a pool (120 cm in diameter) was prepared with white plastic, and the water temperature was maintained at 20°C. Swimming paths were analyzed by a computer system with a video camera (AXIS-90 Target/2; Neuroscience). In the hidden-platform test, the platform (7 cm in diameter) was submerged 1 cm below the water surface. Mice did not swim in the pool before training. Three starting positions were used pseudorandomly, and each mouse was trained with three trials per day for 6 d. After reaching the platform, the mouse was allowed to remain on it for 30 s. If the mouse did not find the platform within 60 s, the trial was terminated and the animal was put on the platform for 30 s. In the platform transfer test, the mouse swam for 60 s in the pool without the platform. In the visible-platform test, the black platform was located 1 cm above the water surface.

For the fear conditioning task, a mouse was placed in a training cage

(25 × 30 × 11 cm), which consisted of transparent Plexiglas with a grid floor for footshock, and the freezing response as the immobility time was measured for 2 min in the absence of sound and footshock (preconditioning) using Scanet SV-10AQ (Toyo Sangyo), which can measure automatically the immobility time by digital counters with infrared sensors. In the conditioning, the mouse was again placed in the cage, and the pretrial time of 2 min was followed by a 15 s tone stimulus (80 dB). During the last 5 s of the tone stimulus, a footshock of 0.8 mA was delivered through a shock generator (NS-SG01; Neuroscience). This procedure was repeated four times with 15 s intervals. In the pseudoconditioning, the mouse was exposed to the conditioning without footshock. For the contextual test 24 h after the conditioning, the mouse was placed back in the same cage in the absence of sound and footshock. For the cued test 24 h after the conditioning, the mouse was placed in a novel cage (45 × 26 × 40 cm), which was made of a transparent acrylic cage with a black Plexiglas floor, in the presence of a continuous tone stimulus.

For the novel object recognition task, a mouse was habituated to a black plastic cage (30 × 30 × 50 cm) for 3 d. In the training, two novel objects were placed in the cage, and the mouse was allowed to explore freely for 5 min. Time spent exploring each object was recorded manually. In retentions 2 or 24 h after the training, the mouse was placed back in the same cage, in which one of the familiar objects used in the training was replaced by a novel object, and allowed to explore for 5 min. Exploratory preference, a ratio of time spent exploring any one of the two objects (training) or the novel one (retention) over the total time spent exploring both objects, was used to measure recognition memory.

Electrophysiological analysis. Mouse brains were removed and kept in artificial CSF (ACSF) (in mM: 128 NaCl, 1.7 KCl, 26 $NaHCO_3$, 1.2 KH_2PO_4, 2.4 $CaCl_2$, 1.3 $MgSO_4$, and 10 glucose). ACSF was saturated with a mixture of 95% O_2/5% CO_2. Slices of the hippocampus (350 μm) were prepared using a microslicer (DTK-1500; Dosaka EM, Kyoto, Japan) and placed for 1 h in an incubation chamber filled with ACSF. The slices were stained with a voltage-sensitive dye, RH 482 (0.1 mg/ml; Nippon Kanko-Shikiso Kenkyusho, Okayama, Japan). The stained slices were transferred to a recording chamber mounted on an inverted microscope (IMT-2; Olympus, Tokyo, Japan). The recording chamber was continuously perfused with ACSF. The optical recording system (HR Deltaron 1700; Fuji Photo Film) consists of an area sensor with 128 × 128 photodiodes and a data-processing unit. Each photodiode receives optical signals from a 25 × 25 μm sample area, thus creating a 3.3 × 3.3 mm recording field. For optical recordings, an ACSF-filled glass electrode was placed in the hippocampal CA3 area. Schaffer collateral afferents were then stimulated with 300 μA/200 μs pulses, and a test stimulus was delivered at 0.06 Hz by a stimulator (SEN-3301; Nihon Kohden, Tokyo, Japan). In each trial, background signals were recorded for 10 ms before the electrical stimulus and stored as a reference image. Images after the stimulus were recorded at 0.6 ms/frame, and the difference signals from the reference image were digitized into 8 bit signals. The digitized signals were then amplified 400 times. To improve the signal-to-noise ratio, 16 trial images were averaged into a single image. A total of 150 sequential images, corresponding to a ~90 ms recording time, were collected from one experiment. The level of neuronal activities was indicated with pseudocolor (256 colors). To analyze the time course of activities in a given sample area, data from each pixel were stored, retrieved, and plotted as a function of time using Origin 5.0 (OriginLab, Northampton, MA).

In vitro *kinase assay.* Immunoprecipitates from the hippocampus were suspended in Src kinase reaction buffer (in mM: 100 Tris-HCl, pH 7.5, 125 $MgCl_2$, 25 $MnCl_2$, 2 EGTA, 0.2 sodium orthovanadate, and 2 dithiothreitol). The kinase assay was performed using a Src kinase kit (catalog #17-131; Upstate Biotechnology).

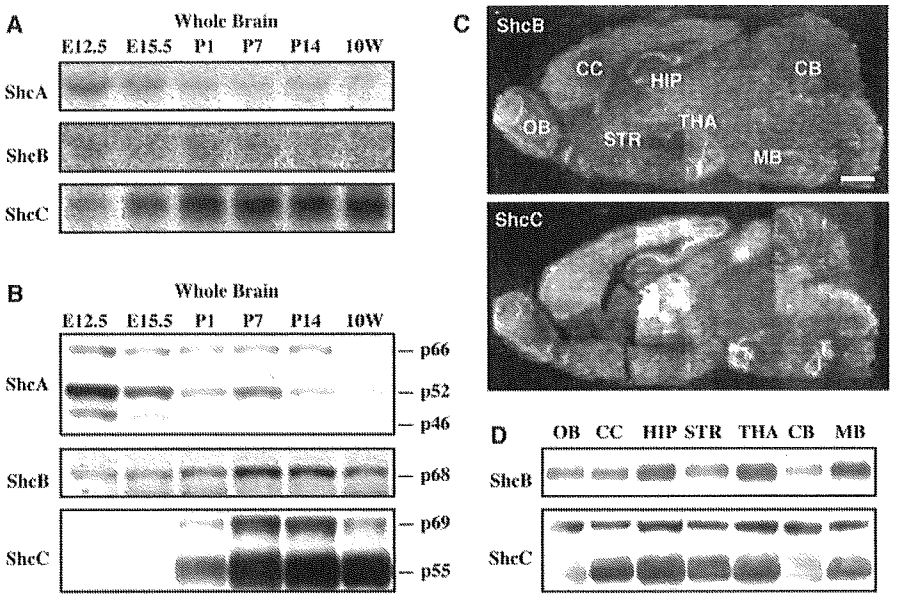

Figure 1. Expression profiles of Shc family members in the brain. ***A***, mRNA expression of Shc family members during brain development. Total RNAs from whole brain in various developmental stages were examined by Northern blot analysis. ***B***, Protein expression of Shc family members during brain development. Protein extracts from whole brain in various developmental stages were examined by Western blot analysis. ***C***, mRNA expression of ShcB and ShcC in the mature brain [10 weeks of age (10W)]. mRNAs were examined by *in situ* hybridization analysis. Scale bar, 1 mm. ***D***, Protein expression of ShcB and ShcC in various regions of the mature brain (10W). Protein extracts from various regions of the brain were examined by Western blot analysis. E12.5 and E15.5, Embryonic days 12.5 and 15.5; OB, olfactory bulb; CC, cerebral cortex; HIP, hippocampus; STR, striatum; THA, thalamus; CB, cerebellum; MB, midbrain.

Pharmacological treatment of tissue slices. The hippocampi were quickly dissected and sliced in two directions at a thickness of 350 μm using a McIlwain tissue chopper (Mickle Laboratory Engineering, Gomshall, UK). The hippocampal slices were incubated at 37°C for 1 h in the netwell chamber (Corning, Corning, NY) filled with ACSF, which was continuously saturated with a mixture of 95% O_2/5% CO_2, and then exposed to ACSF in the presence of glutamate (100 μM), glycine (10 μM), and spermidine (1 mM) for 5 min. After a wash in ice-cold ACSF, the slices were homogenized in the modified lysis buffer.

Statistical analysis. All of the data were expressed as mean ± SEM. Statistical differences between the mutant mice and the wild-type mice were determined with Student's *t* comparison test. In the analysis of the visible or hidden test in the Morris water maze test, statistical differences were determined by an ANOVA with repeated measures. In the analysis of the transfer test in the Morris water maze, fear conditioning, and novel object recognition tasks, statistical differences among values for individual groups were determined by ANOVA, followed by the Student–Newman–Keuls multiple comparisons test when *F* ratios were significant ($p < 0.05$).

Results

ShcC/N-Shc, a major phosphotyrosine adapter protein in the mature hippocampus

The gene expression of Shc-related phosphotyrosine adapter proteins was under dynamic regulation during the mammalian brain development (Fig. 1*A*,*B*). The expression level of ShcA, both the mRNA and protein, decreased during perinatal development and almost disappeared by 10 weeks of age. In contrast, that of ShcC increased gradually during postnatal development, with a peak at approximately postnatal day 7 (P7) to P14. However, ShcB mRNA levels remained low and invariable at all of the developmental stages, whereas its protein levels existed relatively high at P7 and P14. *In situ* hybridization analysis of young adults at 10

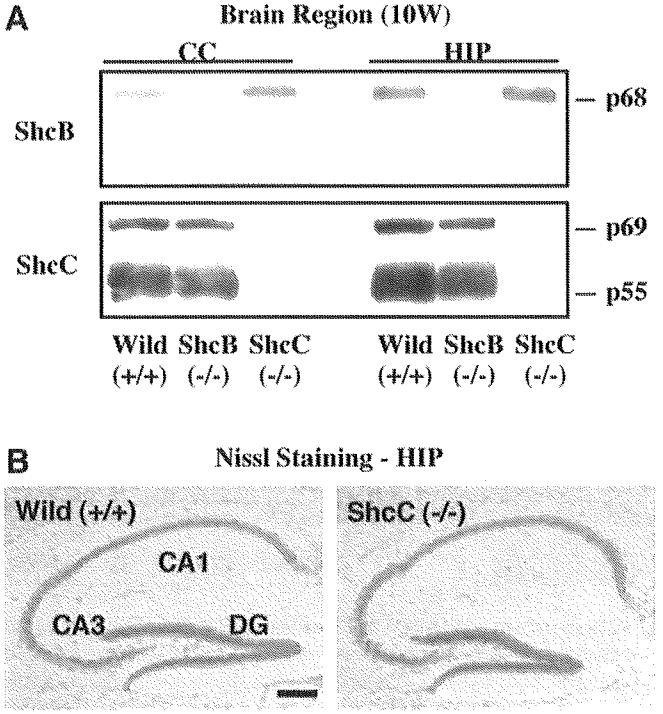

Figure 2. Hippocampal morphology in ShcC mutant mice. ***A***, Protein expression of ShcB and ShcC in ShcC mutant mice [10 weeks of age (10W)]. Protein extracts from the cerebral cortex (CC) and hippocampus (HIP) of ShcB and ShcC mutant mice were examined by Western blot analysis. ***B***, Nissl staining in the hippocampus of ShcC mutant mice (10W). DG, Dentate gyrus. Scale bar, 200 μm.

weeks of age revealed that ShcC mRNA was highly expressed in the cerebral cortex, hippocampus, and thalamus (Fig. 1*C*). In contrast, the expression of ShcB mRNA was rather ubiquitous (Fig. 1*C*). The regional expression of ShcC protein correlated with the mRNA data, whereas that of ShcB protein was different from mRNA and showed some deviations (i.e., a few high expressions in the hippocampus, thalamus, and midbrain) (Fig. 1*D*). The expression of ShcA was negligible in the various regions of the brain at 10 weeks of age (data not shown). These findings indicate that ShcC is the primary phosphotyrosine adapter protein among the Shc family members in the hippocampus of adult animals.

Histological appearance of hippocampal neurons in ShcC mutant mice

ShcC mutant mice exhibited a complete loss of ShcC protein, but the expression of ShcB was unaffected in most regions of the brain at 10 weeks of age (Fig. 2*A*, cerebral cortex and hippocampus). Neuroanatomically, the hippocampus of ShcC mutant mice revealed no gross structural abnormalities on Nissl staining compared with that of wild-type mice (Fig. 2*B*). MAP2 immunostaining for the dendrites of neurons in the hippocampal CA1 area of the mutant mice gave a pattern indistinguishable from that in wild-type mice (data not shown). Thus, the deficiency of ShcC did not significantly alter the hippocampal morphology in the mature brain.

Enhancement of hippocampus-dependent learning and memory in ShcC mutant mice

To investigate whether a deficiency of ShcC affects neuronal functions of the mature brain, we examined the performance of ShcC mutant mice in several behavioral paradigms. We first tested motor coordination and nociceptive response. The motility in a novel environment was measured for both horizontal (locomotion) and vertical (rearing) activities. Neither locomotion nor rearing during a 60 min observation period differed significantly between the wild-type mice (locomotion, 13,122.2 ± 1197.8 counts; rearing, 70.7 ± 13.8 counts) and ShcC mutant mice (locomotion, 13,355.0 ± 1405.0 counts; rearing, 81.8 ± 14.1 counts). Furthermore, no aberrant nociceptive responses to electric footshocks were observed in the ShcC mutant mice: the footshock threshold in the mutant mice (flinching, 0.045 ± 0.002 mA; vocalizing, 0.233 ± 0.027 mA; jumping, 0.425 ± 0.031 mA) was the same as that in wild-type mice (flinching, 0.045 ± 0.004 mA; vocalizing, 0.228 ± 0.015 mA; jumping, 0.400 ± 0.046 mA). These results indicate no apparent abnormalities in either motor or sensory neuronal systems in the ShcC mutant mice, consistent with previous observations (Sakai et al., 2000).

We next tested spatial and nonspatial learning and memory in ShcC mutant mice using the paradigms of the Morris water maze, fear conditioning, and novel object recognition tasks. In the Morris water maze task, both the wild-type and ShcC mutant mice managed to learn the visible-platform test, but the escape latency to the platform was shorter for the mutant mice (ANOVA with repeated measures; $F_{(1,22)} = 4.446$; $p = 0.0010$) (Fig. 3*Aa*). In the hidden-platform test, which requires the activation of the NMDA receptors in the hippocampus (Morris et al., 1982; Tsien et al., 1996), ShcC mutant mice required less time to reach the platform than wild-type mice (ANOVA with repeated measures; $F_{(1,34)} = 3.689$; $p = 0.0034$) (Fig. 3*Ab*). Swimming speeds of the wild-type and ShcC mutant mice in the visible- and hidden-platform tests were essentially the same (swimming speed on the first day of the hidden-platform test; wild-type mice, 17.9 ± 1.2 cm/s; ShcC mutant mice, 18.6 ± 1.1 cm/s). Moreover, in the platform transfer test conducted after the hidden-platform test, the ShcC mutant mice exhibited greater preference for the trained quadrant than the wild-type mice (Fig. 3*Ac*).

We tested for associative memory in the contextual and cued fear conditioning tasks. The former is hippocampus dependent, whereas the latter is hippocampus independent (Phillips and LeDoux, 1992). Both types of fear conditioning task also require the activation of the NMDA receptors (Davis et al., 1987; Kim et al., 1992). The contextual and cued fear conditioning tasks were measured 24 h after an aversive event (footshock) using two separate sets of genotype groups. The freezing response before the footshock (preconditioning) did not differ between the wild-type and ShcC mutant mice (Fig. 3*B*). In the contextual fear conditioning test, the freezing response 24 h after the footshock in both the wild-type and ShcC mutant mice significantly increased compared with the preconditioning and pseudoconditioning groups, respectively, with the mutant mice exhibiting a much stronger response than wild-type mice (Fig. 3*B*). In contrast, in the cued fear conditioning test, there was no significant difference in the freezing response 24 h after the footshock between the wild-type mice (62.6 ± 5.1%) and ShcC mutant mice (64.6 ± 3.3%).

To examine visual recognition memory in ShcC mutant mice, we used a novel object recognition task, in which the activation of the NMDA receptors in the hippocampus is essential for the formation of recognition memory (Rampon et al., 2000). We used a 5 min training protocol to assess the enhancement of learning and memory. There was no difference in exploratory preference during the training between the wild-type and ShcC mutant mice (Fig. 3*C*), indicating that the two groups essentially had the same levels of curiosity and/or motivation to explore the two objects.

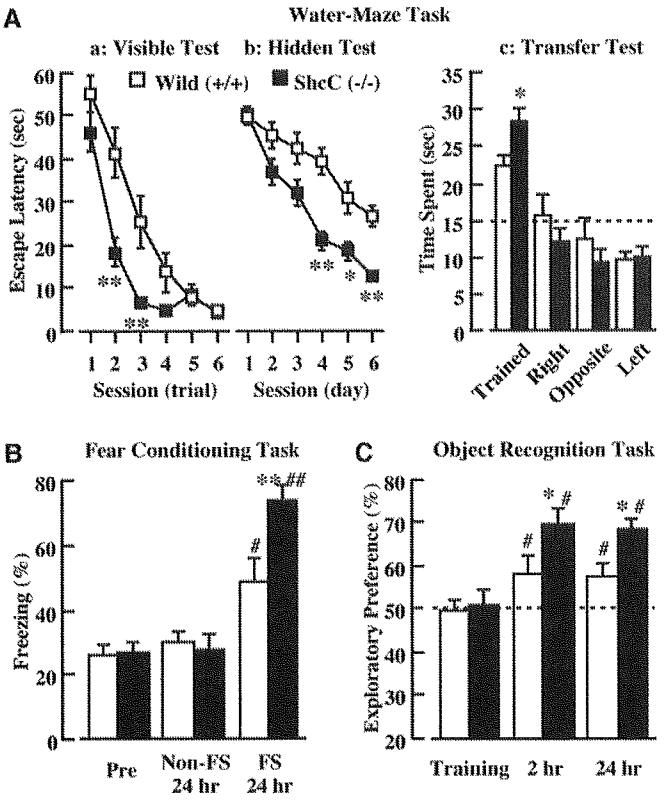

Figure 3. Hippocampus-dependent learning and memory in ShcC mutant mice. ***A***, Morris water maze task. Escape latency in the visible (***a***)- and hidden (***b***)-platform tests. ***c***, The time spent in each quadrant in the transfer test 24 h after the hidden-platform test. The time spent in the trained quadrant was significantly longer than that in any other quadrants in both the wild-type and ShcC mutant mice ($p < 0.05$; Student–Newman–Keuls multiple comparisons test). The dotted line represents performance by chance (15 s). ***B***, Contextual fear conditioning test. The freezing response was measured for 2 min 24 h after the conditioning [FS (footshock)] or pseudoconditioning (Non-FS). ***C***, Novel object recognition test. The time spent exploring two objects was measured for 5 min during training and retention 2 or 24 h after the training. The dotted line represents performance by chance (50%). Data represent mean ± SEM (n = 8–18). $^{*}p < 0.05$ and $^{**}p < 0.01$ versus corresponding wild type (+/+). $^{\#}p < 0.05$ and $^{\#\#}p < 0.01$ versus corresponding non-FS or training value in wild type (+/+).

In 2 and 24 h retention, however, ShcC mutant mice exhibited greater preference toward the novel object than wild-type mice (Fig. 3*C*).

Overall, these findings in the three different paradigms suggest that hippocampus-dependent spatial and nonspatial learning and memory is enhanced in the ShcC mutant mice, and this enhancement reflects neither increased motor activity nor altered nociceptive sensitivity.

Enhancement of hippocampal LTP in ShcC mutant mice

To investigate the synaptic properties in the hippocampus of ShcC mutant mice, we performed electrophysiological analyses using hippocampal slices. We used a high-speed optical recording technique in the hippocampal CA1 area by stimulating Schaffer collateral afferents from the CA3 area. With this technique, the optical signals evoked in the stratum radiatum of the CA1 area were broken down into two distinct elements, an initial spike-like component and an immediately following slow component, which could be separated by a notch in the control (Fig. 4*Aa*, arrow). These components represent the presynaptic fiber volley (PSFV) and EPSP, respectively, because the spike-like component left in Ca^{2+}-free medium (Fig. 4*Ab*) is eliminated by tetrodotoxin (TTX; 1 μM) (Fig. 4*Ad*) and the slow component is

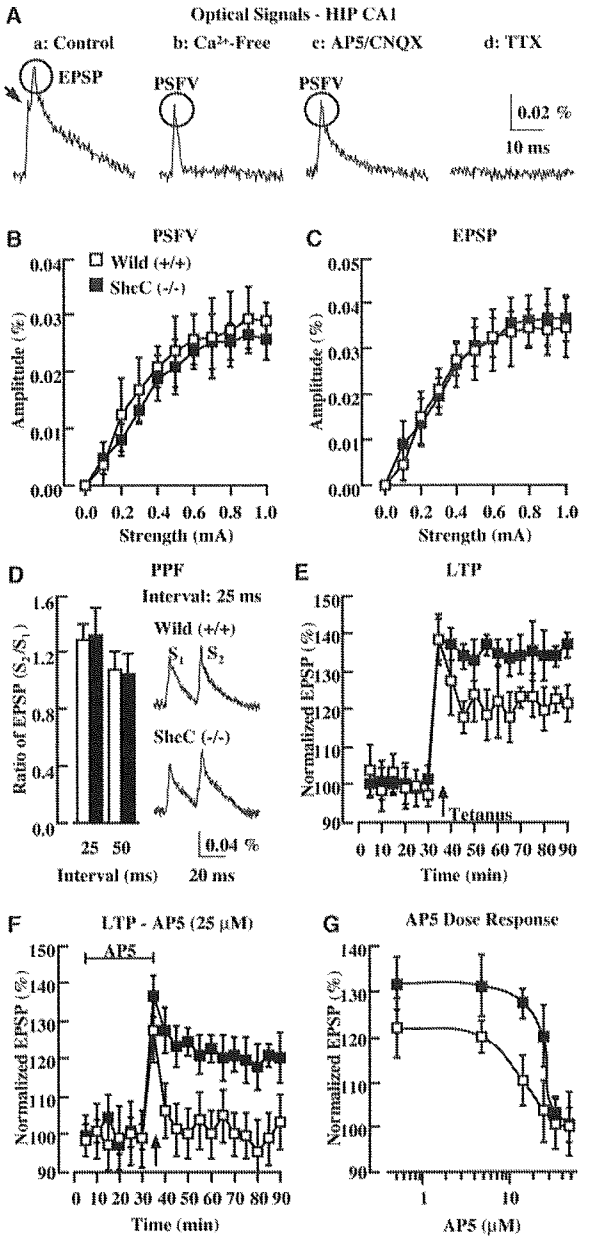

Figure 4. Hippocampal synaptic transmission and LTP in ShcC mutant mice. ***A***, Optical signals in the stratum radiatum of the hippocampal (HIP) CA1 area. Representative traces of optical signal in response to an electrical stimulus of the Schaffer collateral fibers are shown. The control signal (***a***) is composed of PSFV (arrow) and EPSP: the former could be separated by treatment with Ca^{2+}-free medium (***b***) or AP-5 (50 μM)/CNQX (10 μM) (***c***) and eliminated by treatment with TTX (1 μM) (***d***). ***B***, Amplitude of PSFV versus stimulus intensity. ***C***, Amplitude of EPSP versus stimulus intensity. The input–output relationship of PSFV or EPSP is plotted against stimulus intensity at the Schaffer collateral-CA1 synapses (5 slices from 4 wild-type mice; 5 slices from 5 ShcC mutant mice). ***D***, Paired-pulse facilitation (PPF). The data represent the facilitation of the second EPSP (S_2) relative to the first EPSP (S_1). Traces are the synaptic responses evoked by paired-pulse stimulation (interval, 25 ms) (4 slices from 3 wild-type mice; 4 slices from 3 ShcC mutant mice). ***E***, Hippocampal LTP. Each point represents the mean ± SEM EPSP normalized to the baseline EPSP, which was the mean of EPSP for 20–30 min (7 slices from 4 wild-type mice; 7 slices from 4 ShcC mutant mice). Tetanic stimulation induced LTP at 90 min in the wild-type mice (121.2 ± 5.0%) and ShcC mutant mice (136.8 ± 3.4%; $p < 0.05$). ***F***, Treatment with NMDA receptor antagonist AP-5. Each point represents the normalized mean of EPSP ± SEM in the presence of AP-5 (25 μM) for 5–35 min (4 slices from 4 wild-type mice; 6 slices from 4 ShcC mutant mice). Tetanic stimulation with AP-5 treatment failed to induce LTP in the wild-type mice (103.5 ± 7.0% at 90 min), and induced LTP in ShcC mutant mice (120.1 ± 6.7% at 90 min; $p < 0.05$). ***G***, Dose–effect of AP-5 on LTP expression. Each point represents the normalized mean ± SEM EPSP at 60 min after the tetanic stimulation in the presence of different concentrations of AP-5 (4 slices from 4 wild-type mice; 6 slices from 4 ShcC mutant mice) (EC_{50}; wild-type mice, 15.2 μM; ShcC mutant mice, 26.6 μM).

blocked by D-2-amino-5-phosphonovaleric acid (AP-5; 50 μM)/6-cyano-7-nitroquinoxaline-2,3-dione (CNQX; 10 μM), competitive NMDA and AMPA receptor antagonists (Fig. 4*Ac*).

Initial experiments were designed to examine the input–output relationship of synaptic transmission by measuring two distinct components for a range of stimulus intensities. The amplitude of PSFV in the wild-type and ShcC mutant mice was almost the same (Fig. 4*B*), indicating that presynaptic properties were not altered in the mutant mice. There was no difference in the amplitude of EPSP between the wild-type and ShcC mutant mice (Fig. 4*C*), indicating that basal synaptic transmission remains normal in the mutant mice. Similarly, paired-pulse facilitation, which is a short-term enhancement of synaptic efficacy in response to a closely spaced second stimulus and reflects the probability of neurotransmitter release from afferent neurons, differed little between the wild-type and ShcC mutant mice (Fig. 4*D*). These results suggest that synaptic transmission does not deteriorate at the hippocampal Schaffer collateral-CA1 synapses in the ShcC mutant mice.

The LTP in the hippocampal CA1 area, a typical form of synaptic plasticity, is known to involve the activation of the NMDA receptors in its induction. We next examined the synaptic plasticity at hippocampal CA1 synapses using a high-frequency conditioning, tetanic stimulation (100 Hz; 1 s) to induce LTP. There was a marked difference in the expression of hippocampal LTP between the wild-type and ShcC mutant mice (Fig. 4*E*). The early phase of LTP in ShcC mutant mice was consistently enhanced during observation up to 60 min after the tetanic stimulation (wild-type mice, 121.2 ± 5.0%; ShcC mutant mice, 136.8 ± 3.4%; $p < 0.05$) (Fig. 4*E*, EPSP at 90 min). The treatment with AP-5 (25 μM) before the tetanic stimulation in wild-type mice completely blocked the expression of LTP, whereas that in ShcC mutant mice induced LTP (EPSP at 90 min) (wild-type mice, 103.5 ± 7.0%; ShcC mutant mice, 120.1 ± 6.7%; $p < 0.05$) (Fig. 4*F*). As shown in Figure 4*G*, AP-5 dose-dependently inhibited the expression of LTP in both the wild-type and ShcC mutant mice, but with different EC_{50} values of AP-5 between the two groups (wild-type mice, 15.2 μM; ShcC mutant mice, 26.6 μM). These results suggest that the enhancement of hippocampal LTP in ShcC mutant mice would arise from the functional alteration of postsynaptic NMDA receptors in the hippocampal CA1 area, because presynaptic function is normal in this area.

Increased phosphorylation of the NMDA receptors in the hippocampus of ShcC mutant mice

The NMDA receptors are formed by NR1 (GluRζ1) and NR2A to NR2D (GluRε1 to GluRε4) subunits (Hollmann and Heinemann, 1994; Nakanishi and Masu, 1994), and their activity is modulated by either the subunit composition of the receptor (Kutsuwada et al., 1992; Monyer et al., 1994) or phosphorylation of the subunits (Wang and Salter, 1994; Yu et al., 1997). To investigate NMDA receptor activity in the hippocampus of ShcC mutant mice, we examined the expression and phosphorylation levels of the receptor subunits. There was no difference in the expression level of the NR2A, NR2B, or NR1 subunit in the hippocampus between the wild-type and ShcC mutant mice (Fig. 5*A*). The expression level of PSD95, which regulates the signaling by the NMDA receptors, was the same in ShcC mutant mice as in wild-type mice (Fig. 5*A*). However, the tyrosine phosphorylation level of NR2A or NR2B in ShcC mutant mice showed a significant increase compared with that in wild-type mice (Fig. 5*A*). These findings suggest that the basal function of the NMDA receptors in the hippocampus of ShcC mutant mice is enhanced by the hyperphosphorylation at tyrosine residues of the receptor subunits.

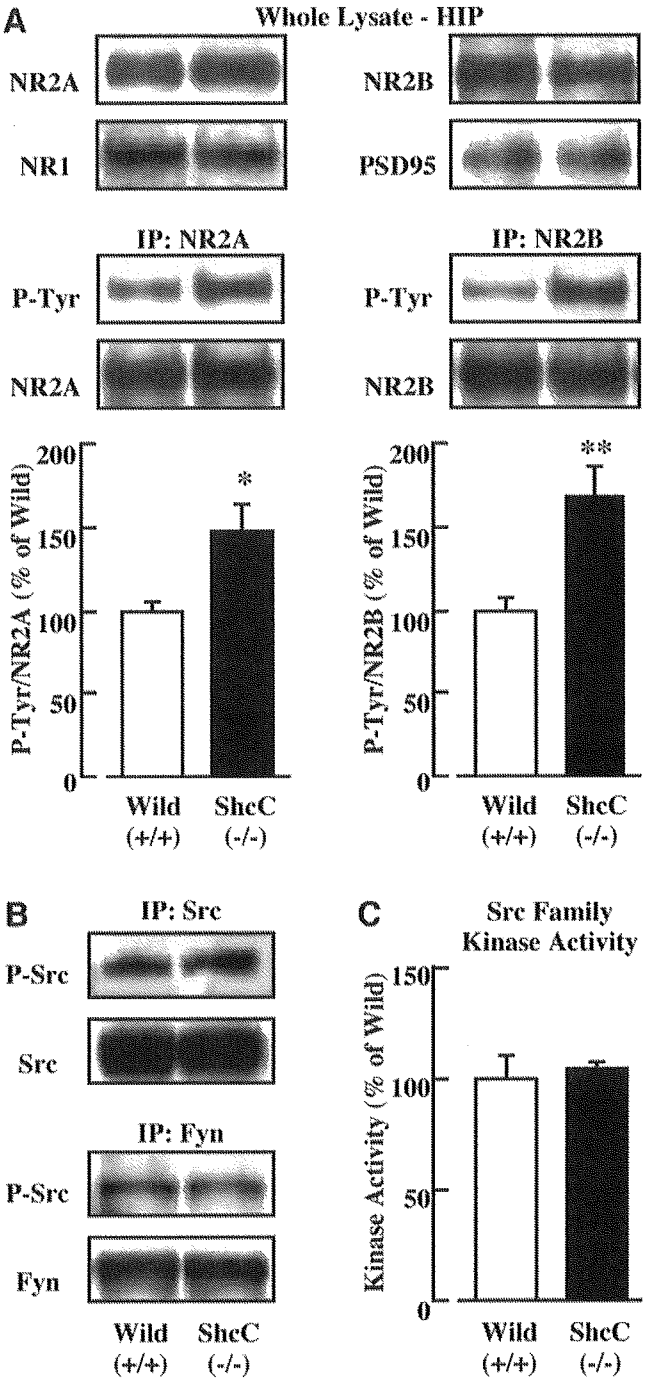

Figure 5. Phosphorylation of the NMDA receptors and kinase activity of the Src family in the hippocampus of ShcC mutant mice. ***A***, Expression and tyrosine phosphorylation of the NR2A and NR2B subunits. The whole lysates of the hippocampus (HIP) were immunoblotted with anti-NR2A, -NR2B, -NR1, or -PSD95 antibody. To dissociate the NMDA receptor complex, hippocampal lysates with a modified lysis buffer were boiled for 5 min. The immunoprecipitates (IP) obtained with anti-NR2A or -NR2B antibody were immunoblotted with anti-phosphotyrosine (P-Tyr) antibody. ***B***, Tyrosine phosphorylation at the activation site of Src and Fyn. The immunoprecipitates prepared with anti-Src or -Fyn antibody were immunoblotted with anti-phospho-Src (P-Src) family antibody. ***C***, Kinase activity of the Src family *in vitro*. The immunoprecipitates obtained with anti-Src family antibody were subjected to an *in vitro* Src kinase assay. Data represent mean ± SEM ($n = 4$). *$p < 0.05$ and **$p < 0.01$ versus corresponding wild type (+/+).

Because the tyrosine phosphorylation of subunits NR2A and NR2B of the NMDA receptors is known to be modulated by the

Src family of cytoplasmic tyrosine kinases, including Src and Fyn (Hisatsune et al., 1999; Nakazawa et al., 2001), we tested the kinase activity of this family in the hippocampus of ShcC mutant mice. However, there was no notable difference in the tyrosine phosphorylation level at the activation site of Src or Fyn between the wild-type and ShcC mutant mice (Fig. 5*B*). Moreover, the kinase activity of the Src family in the mutant mice was similar to that in wild-type mice (Fig. 5*C*). These results indicate that increased tyrosine phosphorylation of the NMDA receptors in the ShcC mutant mice is not attributable to the activation of Src and Fyn.

Interaction of ShcC/N-Shc with the NMDA receptors and the Src family in the hippocampus

To clarify the regulatory mechanism of ShcC in NMDA receptor function involved in hippocampal synaptic plasticity, we investigated whether ShcC interacts with the NMDA receptors and the Src family. In an immunoprecipitation assay using lysates prepared from the hippocampus of wild-type mice, the NR1 or NR2B subunit of the NMDA receptors coprecipitated greatly with ShcC compared with other Shc family members (Fig. 6*A*). Similarly, Src (or Fyn) also interacted with ShcC (Fig. 6*A*). To further test whether these interactions would be affected by the activation of excitatory synaptic transmission, we examined the interaction between ShcC and the NR2B subunit or the Src family under conditions of glutamate stimulation in hippocampal slices from wild-type mice. After a 5 min stimulation with glutamate (100 μM) in the presence of glycine (10 μM) and spermidine (1 mM), both endogenous coactivators for the NMDA receptors, the amount of NR2B subunit coimmunoprecipitated with ShcC increased significantly (Fig. 6*B*). In the same conditions, the interaction of Src (or Fyn) with ShcC also increased significantly (Fig. 6*B*). These findings indicate that ShcC binds to the NMDA receptors and also associates with Src and/or Fyn in the mature hippocampus, and the formation of this ternary complex is stimulated by the activation of the excitatory glutamatergic neuronal system.

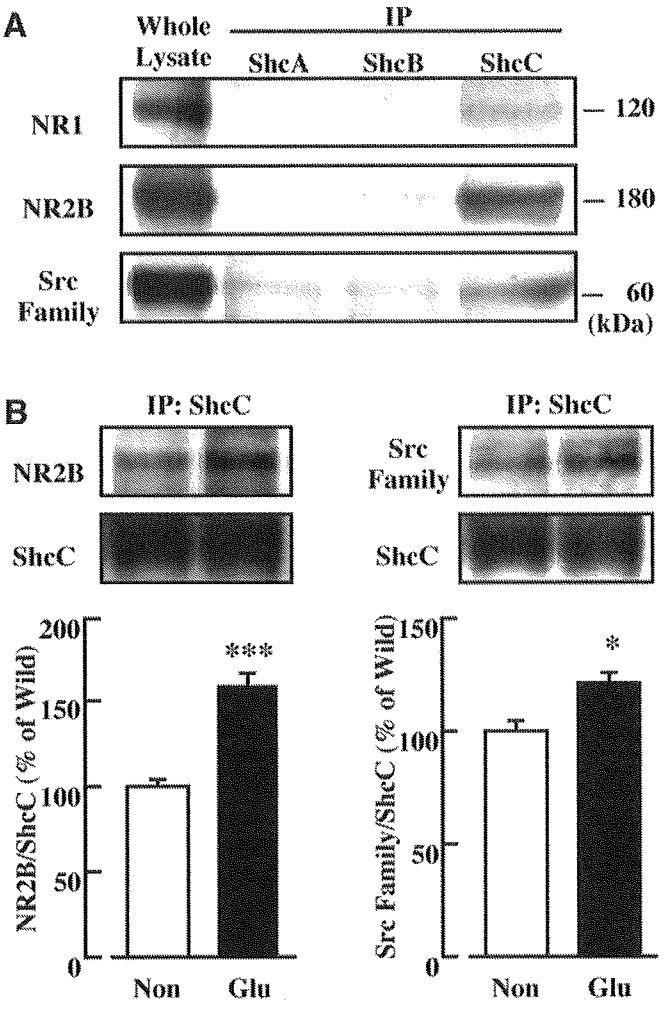

Figure 6. Interaction of ShcC with the NMDA receptors and the Src family in the hippocampus. ***A***, Coimmunoprecipitation with Shc family members in the hippocampus. The immunoprecipitates (IP) obtained with antibodies for ShcA, ShcB, or ShcC were immunoblotted with anti-NR1, -NR2B, or -Src family antibody. ***B***, Coimmunoprecipitation with ShcC in the hippocampus after glutamate (Glu) stimulation. Hippocampal slices were treated with glutamate (100 μM)/glycine (10 μM)/spermidine (1 mM) for 5 min. The immunoprecipitates (IP) prepared with anti-ShcC antibody were immunoblotted with anti-NR2B or -Src family antibody. Data represent mean ± SEM ($n = 4$). $^*p < 0.05$ and $^{***}p < 0.001$ versus corresponding wild type (+/+).

Discussion

In the present study, we demonstrated that the phosphotyrosine adapter protein ShcC/N-Shc is implicated in the modulation of hippocampal synaptic plasticity. However, as described in Introduction, hippocampal LTP may not rely on the Shc-mediated TrkB-Ras/MAPK signaling (Korte et al., 2000; Minichiello et al., 2002). Rather than the Shc/Ras/MAPK pathway, the PLCγ/IP3/CaMKIV pathway may be more relevant to the modulation of hippocampal LTP immediately downstream of the TrkB receptor (Minichiello et al., 2002). Thus, our results were unexpected, and we were interested in the novel role of ShcC to modulate the hippocampal LTP underlying learning and memory. We therefore estimate that the role of ShcC in hippocampal synaptic plasticity is independent of the Ras/MAPK pathway from the TrkB receptor and is critical to the modulation of NMDA receptor function, based on the attenuated effect of an NMDA receptor antagonist on LTP expression and the increased tyrosine phosphorylation of the NMDA receptors in the hippocampus of ShcC mutant mice.

Role of ShcC/N-Shc in hippocampal synaptic plasticity via interaction with the NMDA receptor

We have shown here that ShcC specifically interacted with the NR2B subunit of the NMDA receptors and Src (or Fyn) of tyrosine kinases in the hippocampus, and these interactions were enhanced by glutamate stimulation. The NR2B subunit is phosphorylated at several tyrosine residues by Src and Fyn (Hisatsune et al., 1999; Nakazawa et al., 2001), and the phosphorylation levels are upregulated by tetanic stimulation to induce hippocampal LTP (Rosenblum et al., 1996; Rostas et al., 1996). Thus, it is plausible that ShcC affects NMDA receptor function by binding to the receptor subunit via its phosphotyrosine binding property in an activity-dependent manner. Therefore, ShcC would regulate the receptor activation in the hippocampal LTP through Src family kinase-mediated tyrosine phosphorylation.

The elevated tyrosine phosphorylation levels of NMDA receptor subunits and normal kinase activity levels of the Src family in the hippocampus of ShcC mutant mice suggest that ShcC is implicated in the dephosphorylation of the receptor subunits. If the phosphorylation of the NMDA receptors is downregulated in the presence of ShcC, a potential role of ShcC could be to recruit a certain protein tyrosine phosphatase to the receptor multicomplex or to activate directly or indirectly a phosphatase for phosphotyrosine residues on the receptor subunits. Thus, ShcC binds

the phosphorylated NMDA receptor subunits and also may modulate the dephosphorylation status of the receptor subunits. Alternatively, if the NMDA receptor phosphorylation is upregulated in the presence of ShcC, the interaction of ShcC with a phosphorylated tyrosine of the receptor subunits may mask other tyrosine residues on the subunits from additional phosphorylation by the Src family. Otherwise, ShcC may inhibit activation of an unknown tyrosine kinase for the receptor subunits. Therefore, ShcC would contribute to the interaction between Src-like tyrosine kinase and a tyrosine phosphatase around the NMDA receptor multicomplex, to modulate the hippocampal synaptic plasticity via the receptor activation.

In general, synaptic plasticity is considered a leading candidate for a cellular mechanism of learning and memory (Bliss and Collingridge, 1993; Malenka and Nicoll, 1999), and a good correlation between NMDA receptor-dependent LTP and spatial learning and memory has been demonstrated (Tsien et al., 1996; Tang et al., 1999). Therefore, the superior hippocampus-dependent learning and memory in ShcC mutant mice would be primarily caused by the enhanced NMDA receptor-dependent hippocampal LTP. As evidence to support the above estimation, the difference in the performance of ShcC mutant mice between the contextual and cued fear conditioning tasks should be mentioned. The contextual associative memory is hippocampus dependent, whereas the cued associative memory is hippocampus independent (Phillips and LeDoux, 1992). Both associative memories also depend on the amygdala (Lavond et al., 1993) and NMDA receptor activation (Davis et al., 1987; Kim et al., 1992). Thus, the enhancement of only the former in ShcC mutant mice suggests the specific activation of the NMDA receptors in the hippocampus of the mutant mice.

However, the enhancement of behavioral performance in ShcC mutant mice was observed not only in the hidden-platform test of the Morris water maze task that depends on the hippocampus but also in the visible-platform test that is not necessarily hippocampus dependent. Thus, the performance of ShcC mutant mice in the present behavioral tasks may not be affected by only a specific improvement of hippocampus-dependent learning and memory. There are several explanations for the better performance of ShcC mutant mice in the latter test (e.g., the alteration of motility, emotionality, and visual acuity). Although there was at least no difference in the motility, especially swimming ability, of ShcC mutant mice, emotionality such as motivation to escape from water may be affected by alterations of NMDA receptor function in the hippocampus, because the alterations are known to influence emotion-associated neuronal circuits in other regions of the brain (e.g., the dopaminergic and serotonergic neuronal systems in the cerebral cortex and striatum) (Mohn et al., 1999; Miyamoto et al., 2001). Currently, there is no evidence that ShcC is involved in emotionality and those neuronal systems. However, because ShcC is expressed in the retinal ganglion cell during perinatal development (Nakazawa et al., 2002), a loss of ShcC may have some influence on the performance of visual acuity. Therefore, there is a need to investigate the emotional and visual performance in ShcC mutant mice.

Upstream and downstream signaling of the ShcC/N-Shc associated with hippocampal synaptic plasticity

We discussed above that ShcC plays a role in the modulation of hippocampal synaptic plasticity via interaction with the postsynaptic NMDA receptors but not with the BDNF-stimulated TrkB receptors. This idea is consistent with the findings that ShcC accumulates in the PSD (Suzuki et al., 1999) and BDNF is required for presynaptic but not postsynaptic modulation of LTP in the hippocampal CA3–CA1 synapses (Xu et al., 2000; Zakharenko et al., 2003). However, it remains possible that ShcC is involved in TrkB-mediated hippocampal synaptic plasticity at the postsynapses, because BDNF was taken up by postsynaptic neurons in an activity-dependent manner (Kohara et al., 2001). Thus, the enhanced hippocampal LTP in ShcC mutant mice may be caused in part by alterations of postsynaptic TrkB receptor signaling, for example, through activation of the PLCγ-mediated TrkB–IP3/CaMKIV pathway that is proposed to be relevant to hippocampal LTP (Minichiello et al., 2002). More studies are needed to clarify the signaling capabilities of the BDNF-stimulated TrkB receptors in the absence of ShcC and the signaling ability of ShcC as a go-between adapter protein for the TrkB and NMDA receptors, because NMDA receptor activation is frequently associated with TrkB-mediated hippocampal LTP (Suen et al., 1997; Levine et al., 1998). In addition, it is essential to investigate directly the NMDA receptor synaptic responses in ShcC mutant mice, because our findings showed only differences in the contribution of NMDA receptor to hippocampal LTP in the mutant mice.

Similarly to ShcC mutant mice, mice lacking H-Ras showed enhanced hippocampal LTP and tyrosine phosphorylation of the NMDA receptors (Manabe et al., 2000). These enhancements explained why the deficiency of H-Ras increased Src kinase activity and subsequently potentiated the receptor function associated with hippocampal LTP (Thornton et al., 2003). These findings might suggest that ShcC modulates NMDA receptor function for hippocampal LTP via inhibition of Src kinase activity through the Ras family, including H-Ras, because ShcC transmits BDNF-stimulated TrkB receptor signaling to the Ras/MAPK pathway (Nakamura et al., 1998; Liu and Meakin, 2002). In this study, however, Src and Fyn kinase activity were unaffected in the hippocampus of ShcC mutant mice, which was distinct from the case of H-Ras mutant mice.

Hippocampal synaptic modulation by ShcC may also involve other molecules. A novel 250 kDa Rho-GTPase activating protein (GAP) Grit (Nakamura et al., 2002), also termed RICS (Rho GAP involved in the β-catenin–N-cadherin and NMDA receptor signaling) (Okabe et al., 2003) or p250GAP (Nakazawa et al., 2003), is suggested to be involved in modulation of NMDA receptor signaling. Grit was identified originally as a binding partner of ShcC and is involved in neurotrophin-dependent neurite outgrowth via the specific modulation of cytoskeletal actin dynamics (Nakamura et al., 2002). Actin dynamics in dendritic spines have been implicated in hippocampal LTP (Engert and Bonhoeffer, 1999; Matus, 2000). Grit interacted with the NR2B subunit of the NMDA receptors, and this interaction was modulated by the receptor activation (Nakazawa et al., 2003). These findings suggest that Grit regulates the NMDA receptor-dependent actin reorganization in dendritic spines. Thus, the absence of ShcC may also influence the localization of Grit and further affect the postsynaptic remodeling of the cytoskeleton underneath the NMDA receptors, which is associated with hippocampal LTP underlying learning and memory (Milner et al., 1998). It could be that multiple molecules are needed to regulate synaptic function for hippocampal LTP (Sanes and Lichtman, 1999; Inoue and Okabe, 2003); however, ShcC would be a modulatory component of these molecules at the hippocampal synapses.

In summary, our observations revealed that the enhancement of hippocampal LTP in ShcC mutant mice is primarily attributable to an alteration of NMDA receptor function rather than an effect on the TrkB–Shc site. The current study established that the

neural-specific phosphotyrosine adapter protein ShcC/N-Shc is a modulator of hippocampal synaptic plasticity underlying learning and memory.

References

Adams JP, Sweatt JD (2002) Molecular psychology: roles for the ERK MAP kinase cascade in memory. Annu Rev Pharmacol Toxicol 42:135–163.

Bliss TV, Collingridge GL (1993) A synaptic model of memory: long-term potentiation in the hippocampus. Nature 361:31–39.

Cattaneo E, Pelicci PG (1998) Emerging roles for SH2/PTB-containing Shc adaptor proteins in the developing mammalian brain. Trends Neurosci 21:476–481.

Davis M, Hitchcock J, Rosen JB (1987) Anxiety and the amygdala: pharmacological and anatomical analysis of the fear-potentiated startle paradigm. In: The psychology of learning and motivation (Bower GH, ed), pp 263–305. New York: Academic.

Engert F, Bonhoeffer T (1999) Dendritic spine changes associated with hippocampal long-term synaptic plasticity. Nature 399:66–70.

Hisatsune C, Umemori H, Mishina M, Yamamoto T (1999) Phosphorylation-dependent interaction of the *N*-methyl-D-aspartate receptor ϵ2 subunit with phosphatidylinositol 3-kinase. Genes Cells 4:657–666.

Hollmann M, Heinemann S (1994) Cloned glutamate receptors. Annu Rev Neurosci 17:31–108.

Inoue A, Okabe S (2003) The dynamic organization of postsynaptic proteins: translocating molecules regulate synaptic function. Curr Opin Neurobiol 13:332–340.

Kaplan DR, Miller FD (2000) Neurotrophin signal transduction in the nervous system. Curr Opin Neurobiol 10:381–391.

Kim JJ, Fanselow MS, DeCola JP, Landeira-Fernandez J (1992) Selective impairment of long-term but not short-term conditional fear by the *N*-methyl-D-aspartate antagonist APV. Behav Neurosci 106:591–596.

Kohara K, Kitamura A, Morishima M, Tsumoto T (2001) Activity-dependent transfer of brain-derived neurotrophic factor to postsynaptic neurons. Science 291:2419–2423.

Kojima T, Yoshikawa Y, Takada S, Sato M, Nakamura T, Takahashi N, Copeland NG, Gilbert DJ, Jenkins NA, Mori N (2001) Genomic organization of the Shc-related phosphotyrosine adapters and characterization of the full-length Sck/ShcB: specific association of p68-Sck/ShcB with pp135. Biochem Biophys Res Commun 284:1039–1047.

Korte M, Minichiello L, Klein R, Bonhoeffer T (2000) Shc-binding site in the TrkB receptor is not required for hippocampal long-term potentiation. Neuropharmacology 39:717–724.

Kutsuwada T, Kashiwabuchi N, Mori H, Sakimura K, Kushiya E, Araki K, Meguro H, Masaki H, Kumanishi T, Arakawa M, Mishina M (1992) Molecular diversity of the NMDA receptor channel. Nature 358:36–41.

Lavond DG, Kim JJ, Thompson RF (1993) Mammalian brain substrates of aversive classical conditioning. Annu Rev Psychol 44:317–342.

Levine ES, Crozier RA, Black IB, Plummer MR (1998) Brain-derived neurotrophic factor modulates hippocampal synaptic transmission by increasing *N*-methyl-D-aspartic acid receptor activity. Proc Natl Acad Sci USA 95:10235–10239.

Liu HY, Meakin SO (2002) ShcB and ShcC activation by the Trk family of receptor tyrosine kinases. J Biol Chem 277:26046–26056.

Lu B (2003) BDNF and activity-dependent synaptic modulation. Learn Mem 10:86–98.

Malenka RC, Nicoll RA (1999) Long-term potentiation—a decade of progress? Science 285:1870–1874.

Manabe T, Aiba A, Yamada A, Ichise T, Sakagami H, Kondo H, Katsuki M (2000) Regulation of long-term potentiation by H-Ras through NMDA receptor phosphorylation. J Neurosci 20:2504–2511.

Matus A (2000) Actin-based plasticity in dendritic spines. Science 290:754–758.

Milner B, Squire LR, Kandel ER (1998) Cognitive neuroscience and the study of memory. Neuron 20:445–468.

Minichiello L, Calella AM, Medina DL, Bonhoeffer T, Klein R, Korte M (2002) Mechanism of TrkB-mediated hippocampal long-term potentiation. Neuron 36:121–137.

Miyamoto Y, Yamada K, Noda Y, Mori H, Mishina M, Nabeshima T (2001) Hyperfunction of dopaminergic and serotonergic neuronal systems in mice lacking the NMDA receptor epsilon1 subunit. J Neurosci 21:750–757.

Mohn AR, Gainetdinov RR, Caron MG, Koller BH (1999) Mice with reduced NMDA receptor expression display behaviors related to schizophrenia. Cell 98:427–436.

Monyer H, Burnashev N, Laurie DJ, Sakmann B, Seeburg PH (1994) Developmental and regional expression in the rat brain and functional properties of four NMDA receptors. Neuron 12:529–540.

Morris RG, Garrud P, Rawlins JN, O'Keefe J (1982) Place navigation impaired in rats with hippocampal lesions. Nature 24:681–683.

Nakamura T, Muraoka S, Sanokawa R, Mori N (1998) N-Shc and Sck, two neuronally expressed Shc adapter homologs. Their differential regional expression in the brain and roles in neurotrophin and Src signaling. J Biol Chem 273:6960–6967.

Nakamura T, Komiya M, Sone K, Hirose E, Gotoh N, Morii H, Ohta Y, Mori N (2002) Grit, a GTPase-activating protein for the Rho family, regulates neurite extension through association with the TrkA receptor and N-Shc and CrkL/Crk adapter molecules. Mol Cell Biol 22:8721–8734.

Nakanishi S, Masu M (1994) Molecular diversity and functions of glutamate receptors. Annu Rev Biophys Biomol Struct 23:319–348.

Nakazawa T, Komai S, Tezuka T, Hisatsune C, Umemori H, Semba K, Mishina M, Manabe T, Yamamoto T (2001) Characterization of Fyn-mediated tyrosine phosphorylation sites on GluR ϵ2 (NR2B) subunit of the *N*-methyl-D-aspartate receptor. J Biol Chem 276:693–699.

Nakazawa T, Nakano I, Sato M, Nakamura T, Tamai M, Mori N (2002) Comparative expression profiles of Trk receptors and Shc-related phosphotyrosine adapters during retinal development: potential roles of N-Shc/ShcC in brain-derived neurotrophic factor signal transduction and modulation. J Neurosci Res 68:668–680.

Nakazawa T, Watabe AM, Tezuka T, Yoshida Y, Yokoyama K, Umemori H, Inoue A, Okabe S, Manabe T, Yamamoto T (2003) p250GAP, a novel brain-enriched GTPase-activating protein for Rho family GTPases, is involved in the *N*-methyl-D-aspartate receptor signaling. Mol Biol Cell 14:2921–2934.

Ohno M, Frankland PW, Chen AP, Costa RM, Silva AJ (2001) Inducible, pharmacogenetic approaches to the study of learning and memory. Nat Neurosci 4:1238–1243.

Okabe T, Nakamura T, Nishimura YN, Kohu K, Ohwada S, Morishita Y, Akiyama T (2003) RICS, a novel GTPase-activating protein for Cdc42 and Rac1, is involved in the β-catenin-N-cadherin and *N*-methyl-D-aspartate receptor signaling. J Biol Chem 278:9920–9927.

Patapoutian A, Reichardt LF (2001) Trk receptors: mediators of neurotrophin action. Curr Opin Neurobiol 11:272–280.

Phillips RG, LeDoux JE (1992) Differential contribution of amygdala and hippocampus to cued and contextual fear conditioning. Behav Neurosci 106:274–285.

Poo MM (2001) Neurotrophins as synaptic modulators. Nat Rev Neurosci 2:24–32.

Rampon C, Tang YP, Goodhouse J, Shimizu E, Kyin M, Tsien JZ (2000) Enrichment induces structural changes and recovery from nonspatial memory deficits in CA1 NMDAR1-knockout mice. Nat Neurosci 3:238–244.

Ravichandran KS (2001) Signaling via Shc family adapter proteins. Oncogene 20:6322–6330.

Rosenblum K, Dudai Y, Richter-Levin G (1996) Long-term potentiation increases tyrosine phosphorylation of the *N*-methyl-D-aspartate receptor subunit 2B in rat dentate gyrus *in vivo*. Proc Natl Acad Sci USA 93:10457–10460.

Rostas JA, Brent VA, Voss K, Errington ML, Bliss TV, Gurd JW (1996) Enhanced tyrosine phosphorylation of the 2B subunit of the *N*-methyl-D-aspartate receptor in long-term potentiation. Proc Natl Acad Sci USA 93:10452–10456.

Sakai R, Henderson JT, O'Bryan JP, Elia AJ, Saxton TM, Pawson T (2000) The mammalian ShcB and ShcC phosphotyrosine docking proteins function in the maturation of sensory and sympathetic neurons. Neuron 28:819–833.

Sanes JR, Lichtman JW (1999) Can molecules explain long-term potentiation? Nat Neurosci 2:597–604.

Silva AJ (2003) Molecular and cellular cognitive studies of the role of synaptic plasticity in memory. J Neurobiol 54:224–237.

Suen PC, Wu K, Levine ES, Mount HT, Xu JL, Lin SY, Black IB (1997) Brain-derived neurotrophic factor rapidly enhances phosphorylation of the postsynaptic *N*-methyl-D-aspartate receptor subunit 1. Proc Natl Acad Sci USA 94:8191–8195.

Suzuki T, Mitake S, Murata S (1999) Presence of up-stream and down-

stream components of a mitogen-activated protein kinase pathway in the PSD of the rat forebrain. Brain Res 840:36–44.

Tang YP, Shimizu E, Dube GR, Rampon C, Kerchner GA, Zhuo M, Liu G, Tsien JZ (1999) Genetic enhancement of learning and memory in mice. Nature 401:63–69.

Thornton C, Yaka R, Dinh S, Ron D (2003) H-Ras modulates NMDA receptor function via inhibition of Src tyrosine kinase activity. J Biol Chem 278:23823–23829.

Tsien JZ, Huerta PT, Tonegawa S (1996) The essential role of hippocampal CA1 NMDA receptor-dependent synaptic plasticity in spatial memory. Cell 87:1327–1338.

Wang YT, Salter MW (1994) Regulation of NMDA receptors by tyrosine kinases and phosphatases. Nature 369:233–235.

Xu B, Gottschalk W, Chow A, Wilson RI, Schnell E, Zang K, Wang D, Nicoll RA, Lu B, Reichardt LF (2000) The role of brain-derived neurotrophic factor receptors in the mature hippocampus: modulation of long-term potentiation through a presynaptic mechanism involving TrkB. J Neurosci 20:6888–6897.

Ying SW, Futter M, Rosenblum K, Webber MJ, Hunt SP, Bliss TV, Bramham CR (2002) Brain-derived neurotrophic factor induces long-term potentiation in intact adult hippocampus: requirement for ERK activation coupled to CREB and upregulation of Arc synthesis. J Neurosci 22:1532–1540.

Yu XM, Askalan R, Keil II GJ, Salter MW (1997) NMDA channel regulation by channel-associated protein tyrosine kinase Src. Science 275:674–678.

Zakharenko SS, Patterson SL, Dragatsis I, Zeitlin SO, Siegelbaum SA, Kandel ER, Morozov A (2003) Presynaptic BDNF required for a presynaptic but not postsynaptic component of LTP at hippocampal CA1–CA3 synapses. Neuron 39:975–990.

Zamanillo D, Sprengel R, Hvalby O, Jensen V, Burnashev N, Rozov A, Kaiser KM, Koster HJ, Borchardt T, Worley P, Lubke J, Frotscher M, Kelly PH, Sommer B, Andersen P, Seeburg PH, Sakmann B (1999) Importance of AMPA receptors for hippocampal synaptic plasticity but not for spatial learning. Science 284:1805–1811.

Crk-Associated Substrate Lymphocyte Type Is Required for Lymphocyte Trafficking and Marginal Zone B Cell Maintenance[1]

Sachiko Seo,* Takashi Asai,* Toshiki Saito,* Takahiro Suzuki,* Yasuyuki Morishita,† Tetsuya Nakamoto,* Motoshi Ichikawa,* Go Yamamoto,* Masahito Kawazu,* Tetsuya Yamagata,* Ryuichi Sakai,‡ Kinuko Mitani,§ Seishi Ogawa,* Mineo Kurokawa,[2]* Shigeru Chiba,* and Hisamaru Hirai*

The lymphocyte-specific Cas family protein Cas-L (Crk-associated substrate lymphocyte type) has been implicated to function in lymphocyte movement, mediated mainly by integrin signaling. However, its physiological role is poorly understood. In this study we analyzed the function of Cas-L in lymphocytes using gene-targeted mice. The mutant mice showed a deficit of marginal zone B (MZB) cells and a decrease of cell number in secondary lymphoid organs. An insufficient chemotactic response and perturbed cell adhesion were observed in Cas-L-deficient lymphocytes, suggesting that the aberrant localization was responsible for the deficit of MZB cells. Moreover, we found that lymphocyte trafficking was altered in Cas-L-deficient mice, which gave a potential reason for contraction of secondary lymphoid tissues. Thus, Cas-L affects homeostasis of MZB cells and peripheral lymphoid organs, which is considered to be relevant to impaired lymphocyte migration and adhesion. *The Journal of Immunology,* **2005, 175: 3492–3501.**

The Crk-associated substrate (Cas)[3] lymphocyte-specific protein Cas-L, also known as human enhancer of filamentation 1 (1), was originally identified as a 105-kDa protein that is tyrosine-phosphorylated by the ligation of β_1 integrin in peripheral T cells (2). Cas-L is a docking protein in focal adhesion and consists of an N-terminal Src homology (SH)3 domain, a substrate domain containing multiple tyrosine motifs for SH2-binding sites, a serine-rich region, and a C-terminal dimerization motif (2). Owing to its homology with p130Cas (3), Cas-L is recognized as a member of the Cas family. Cas is expressed ubiquitously and plays a crucial role in integrin-mediated signaling. Our group demonstrated that the lack of Cas protein resulted in fetal death because of perturbed organogenesis (4). In contrast, Cas-L is predominantly expressed in lymphocytes and epithelial cells (1, 2), which implies that it has distinct functions from Cas.

Integrins are a family of adhesion receptors composed of α and β subunits. They are involved in cell-cell and cell-matrix interactions and induce various biological signals for cell adhesion, migration, apoptosis, proliferation, and differentiation (5–8). Among the integrin family, β_1 integrin constitutes the largest group that mediate cell attachment via fibronectin or VCAM-1. Previous reports showed that Cas-L is tyrosine-phosphorylated by binding to focal adhesion kinase or Pyk-2 in the SH3 domain upon engagement of β_1 integrin (9, 10). Subsequently, the phosphorylated Cas-L regulates several signals involved in cell motility (11–13) and cell adhesion (14) as a downstream effecter of focal adhesion kinase. In addition, Cas-L functions as a signal transducer of TCR (12, 15, 16), BCR (17), and G protein-coupled calcitonin receptor (18). The biological functions of Cas-L in lymphocytes, however, remain to be determined.

Early B cell development arises in bone marrow as immature B cells expressing surface IgM emigrate to the spleen (19). In the spleen, immature B cells can differentiate into follicular B (FOB) cells and marginal zone B (MZB) cells characterized by $IgM^{low}IgD^{high}CD21^{int}CD23^{high}$ and $IgM^{high}IgD^{low}CD21^{high}CD23^{low}$, respectively (20). A number of studies using gene-targeted mice have demonstrated loss of MZB cells in the mutant mice, and this defect of MZB cells was explained by two major mechanisms: failure of MZB cell development and impaired localization. MZB cell development is presumably related to BCR or Notch signal, as suggested from studies of mice lacking Aiolos, Lyn, Notch2, or RBP-J (21–24). The hypothesis of perturbed localization was derived from observations of altered lymphocyte motility in mice lacking Pyk-2, DOCK2, or Lsc (25–27). Despite several investigations, however, the precise mechanism of MZB cell development and localization remains unclear. In particular, no relevant mouse model that recapitulates a defect of integrin-mediated MZB cell retention has been obtained so far.

Lymphocyte trafficking is a multistep process mediated by chemokines and adhesion molecules (28). Lymphocytes express several kinds of chemokine receptors and integrin receptors. The chemokine CXCL12, previously called stromal cell-derived factor

*Department of Hematology and Oncology, Graduate School of Medicine, and †Department of Pathology, Faculty of Medicine, University of Tokyo, Tokyo, Japan; ‡Growth Factor Division, National Cancer Center Research Institute, Tokyo, Japan; and §Department of Hematology, Dokkyo University School of Medicine, Tochigi, Japan

Received for publication January 25, 2005. Accepted for publication July 1, 2005.

The costs of publication of this article were defrayed in part by the payment of page charges. This article must therefore be hereby marked *advertisement* in accordance with 18 U.S.C. Section 1734 solely to indicate this fact.

[1] This work was supported by grants-in-aid from the Ministry of Education, Culture, Sports, Science and Technology of Japan, and the Ministry of Health, Labor and Welfare of Japan.

[2] Address correspondence and reprint requests to Dr. Mineo Kurokawa, Department of Hematology and Oncology, Graduate School of Medicine, University of Tokyo, 7-3-1 Hongo, Bunkyo-ku, Tokyo 113-8655, Japan. E-mail address: kurokawa-tky@umin.ac.jp

[3] Abbreviations used in this paper: Cas, Crk-associated substrate; Cas-L, Cas lymphocyte-type; MZB, marginal zone B; FOB, follicular B; ES, embryonic stem; EGFP, enhanced GFP; TNP, 2,4,6-trinitrophenyl; KLH, keyhole limpet hemocyanin; SH, Src homology.

0022-1767/05/$02.00

1, is integral for mature B cell movement and is expressed in secondary lymphoid tissues, the red pulp in spleen, and the medullary cord in lymph nodes (29, 30). CXCL13, known as B lymphocyte chemoattractant, plays a crucial role in proper localization of B cells in peripheral lymphoid organs (31). With regard to adhesion molecules, previous studies have indicated that the integrin receptors LFA–1 ($\alpha_L\beta_2$) and VLA–4 ($\alpha_4\beta_1$) are involved in lymphocyte homing to peripheral lymph nodes or the splenic white pulp (32–34).

To elucidate the physiological function of Cas-L, we generated Cas-L-deficient mice using gene-targeting strategy. The mutant mice showed reduced numbers of lymphocytes in secondary lymphoid organs and an almost complete loss of MZB cells in the spleen. We demonstrated that Cas-L regulates responses to chemokines and adhesion molecules, and that its deficiency may be related to aberrant peripheral lymphoid organization including MZB cell maintenance.

Materials and Methods

Generation of Cas-L$^{-/-}$ *mice*

A genomic mouse C57BL/6 library was screened with a 300-bp *Cas-L* probe that included the SH3 region of *Cas-L*. A 15-kb clone identified with this probe was subcloned in pBlueScript and all of the genomic sequence was defined. A targeting vector was constructed using the following procedure. The enhanced GFP (pEGFP; Clontech) was directly combined with the *Cas-L* genome at the site of *Hin*dIII within exon 2, and a neomycin resistance cassette was infused to the vector. Electroporation was performed to insert the targeting vector into TT2 embryonic stem (ES) cells. Clones that underwent homologous recombination were selected in the presence of G418 and confirmed by PCR with a primer set containing the left arm. Correctly targeted ES clones were aggregated with eight cell-stage mouse embryos, and male chimeras were crossed with C57BL/6 females to generate mutant mice. To reveal a deficiency of the *Cas-L* gene in mutant mice, Southern blot analysis using the probe indicated was performed (see Fig. 1*A*). Mice were backcrossed with C57BL/6 mice eight times and bred under pathogen-free conditions. Analyses were performed using mainly 8- to 12-wk-old sex-matched littermates.

Western blot analysis

To confirm the deletion of Cas-L protein, thymi from wild-type and *Cas-L*$^{-/-}$ mice were homogenized in cold RIPA buffer (150 mM NaCl, 1% Nonidet P-40, 50 mM Tris (pH 8.0) and 5 mM EDTA-3Na). Cell lysates were incubated with anti-Cas Ab (BD Transduction Laboratories), which cross-reacts to Cas-L, and protein G-Sepharose (Amersham Biosciences) overnight at 4°C. The products of immunoprecipitation were segregated by 7.5% SDS-PAGE. The blotting was conducted with anti-goat human enhancer of filamentation 1 mAb, which developed against a peptide mapping at the N terminus (Santa Cruz Biotechnology).

Cell counts and flow cytometric analysis

Cells from each tissue were washed twice with PBS after hemolysis and enumerated. Peripheral blood was obtained by puncturing the retro-orbital venous plexus and cells were counted using an automatic cell counter (ERMA). Prepared cells were stained with relevant mAbs. Analyses were performed using FACSCalibur (BD Biosciences) and CellQuest software.

Immunohistochemistry

Spleens were frozen in Tissue-Tek OCT compound (Sakura Finetechnical) and cut at 5 μm. Sections were stained with FITC anti-mouse IgD and biotin anti-mouse IgM (BD Pharmingen) diluted to 1/100. IgM expression was detected using Alexa Fluor 594-conjugated streptavidin (Molecular Probes) diluted to 1/250. Confocal laser scanning microscope (Bio-Rad) was used.

Reconstitution of MZB cells

Bone marrow cells (Ly5.2$^+$) were derived from both sides of the femurs, and mononuclear cells were collected using Histopaque (Sigma-Aldrich). Mononuclear cells (1×10^6) in PBS with 10% FCS were i.v. injected into sublethally irradiated (950 rad) 8- to 10-wk-old female wild-type mice with Ly5.1 (C57BL/6). The recipients were sacrificed after 12 wk. The cells of donor origin, separated based on their cell surface expression of Ly5.1 or Ly5.2, were investigated for the presence of MZB cells using FACSCalibur. Fc block was performed by using anti-CD16/32 Abs (BD Pharmingen) to avoid any nonspecific binding of Ly5.

Measurement of intracellular Ca^{2+} concentration

Splenic B cells were purified as described and loaded with 3 μM Indo-1 (Molecular Probes) in RPMI 1640 medium with 1% FCS at 37°C for 45 min. After a rinse of Indo-1, the cells were stained with PerCP anti-mouse B220 (BD Pharmingen) to confirm the B cell fraction. Prepared cells were adjusted to 1×10^7 cells/ml and warmed to 37°C for 5 min. The basal Ca^{2+} concentration was recorded for 30 s. The increase in intracellular free Ca^{2+} after stimulation by 10 μg/ml anti-IgM F(ab′)$_2$ (Jackson ImmunoResearch Laboratories) was subsequently measured for a further 5 min on LSR II (BD Biosciences).

Proliferation assay

Fresh splenocytes were purified by negative selection with MACS microBeads (Miltenyi Biotec). The purified splenic B cells were cultured in 96-well plates (10^5 cells/well) with several concentrations of anti-IgM F(ab′)$_2$ (Jackson ImmunoResearch Laboratories) or with the combination of 3 μg/ml anti-IgM F(ab′)$_2$, 5 μg/ml anti-CD40 (BD Pharmingen), 10 ng/ml recombinant mouse IL-4 (Genzyme/Techne), and 20 μg/ml LPS (Sigma-Aldrich) for 52 h. [^{3}H]Thymidine was added at 1 μCi/well and incubation was done for an additional 8 h.

Immunization and measurement of serum Ig titers

Seven- to 8-wk-old mice were immunized i.p. with 10 μg of 2,4,6-trinitrophenyl keyhole limpet hemocyanin (TNP-KLH; Biosearch Technologies) mixed with alum, given as a booster injection on day 21. Peripheral blood was obtained on day 28. TNP-specific Abs were determined by ELISA with the use of TNP-BSA (LSL). Ten- to 12-wk-old mice were immunized i.p. with 4×10^8 CFU of *Streptococcus pneumoniae* strain R36A, a kind gift of H. Ito, University of Kagoshima (Kagoshima, Japan). Serum was collected on day 7 and the anti-phosphorylcholine-specific Ig levels were measured by ELISA using phosphorylcholine-BSA (Biosearch Technologies). Nonparametric tests were performed on each Ig level.

Migration and adhesion assays

For chemotaxis assays, 5-μm pore-sized transwells (Costar) were used. Splenocytes were stained with CD21, CD23, B220, and Thy1.2. The prepared cells (1.5×10^6) in 100 μl of RPMI 1640 medium were added to the insert, and the bottom chamber was supplied with 450 μl of RPMI 1640 with CXCL12, CXCL13, or CCL21 (Genzyme/Techne) at various concentrations. Migration of the cells to the lower chamber was allowed for 3 h at 37°C. The cells prepared from wild-type or *Cas-L*$^{-/-}$ mice were counted and the number of FOB or T cells was calculated as a control by FACSCalibur. Subsequently, migrated cells were counted and the ratio of FOB or T cells to control cells was calculated. For adhesion assays, erythrocyte-depleted splenocytes on tissue culture plates were incubated at 37°C for 30 min to remove adherent macrophages and stained for CD21, CD23, B220, and Thy1.2. Microtiter wells for adhesion assays were coated with 0.5% BSA, various concentrations of human VCAM-1 (Genzyme/Techne), or recombinant mouse ICAM-1/Fc chimera (R&D Systems) by 1 h incubation at 37°C. Prepared cells (5×10^4 cells/well) were loaded in the precoated wells. After incubation at 37°C for 30 min, control cells in BSA-coated wells were collected and nonadherent cells were discarded. To detach adherent cells, 100 μl of RPMI 1640 medium with 5 mM EDTA and 0.5% BSA was added to each well and the plate was incubated for 15 min on ice. Removed cells were collected and counted on FACSCalibur. Each subset was presented by comparison with the number of the control cells.

Lymphocyte trafficking assay

Splenocytes (Ly5.2$^+$) from 8- to 10-wk-old wild-type or *Cas-L*$^{-/-}$ mice were divided into two portions. One portion was adjusted to a concentration of 4×10^7 cells/ml and labeled with a 3 μM BCECF-AM (2′,7′-bis(carboxyethyl)-4(or 5)-carboxyfluorescein diacetoxymethyl ester; Dojindo Molecular Technologies) solution by incubation at 37°C for 10 min. The other portion was left unlabeled. Labeled cells from *Cas-L*$^{-/-}$ mice and unlabeled cells from wild-type mice were mixed equivalently and injected i.v. into 10- to 12-wk-old female wild-type mice with Ly5.1 (5×10^7 cells/mouse). To eliminate the effect of labeling with BCECF-AM, a complementary experiment was performed simultaneously. After 48 h, cells isolated from spleen, lymph nodes, and peripheral blood of each mouse were stained with Ly5.1, Ly5.2, and CD3 (or B220), and donor cells were separated from recipient cells using Ly5.1 and Ly5.2 by FACSCalibur. To avoid any nonspecific binding of Ly5, Fc block was performed using anti-CD16/32 Abs. The ratio of *Cas-L*$^{-/-}$ cells to control